2024

USING VIRUS LIKE PARTICLE CONJUGATES OF SYNTHETIC TARGETING COMPOUNDS TO DELIVER CHEMOTHERAPEUTIC DRUGS TO CANCER STEM CELLS

Austen W. Kerzee
University of Texas at Tyler, akerzee@patriots.uttyler.edu

USING VIRUS LIKE PARTICLE CONJUGATES OF SYNTHETIC TARGETING COMPOUNDS TO DELIVER CHEMOTHERAPEUTIC DRUGS TO CANCER STEM CELLS

by

AUSTEN W. KERZEE

A thesis submitted in partial fulfillment
of the requirements for the degree of
Masters of Science in Chemistry
Department of Chemistry and Biochemistry

Jiyong Lee, Ph.D., Committee Chair

College of Arts and Sciences

The University of Texas at Tyler
March 2024

The University of Texas at Tyler
Tyler, Texas

This is to certify that the Master's Thesis of

AUSTEN W. KERZEE

has been approved for the thesis requirement on
March 20, 2024 for
the Master of Science degree

Approvals:

DocuSigned by:
Dr. Jiyong Lee
C2E690EC5AFF4E8...
Thesis Chair: Jiyong Lee, Ph.D.

DocuSigned by:
7309BE24D40A4D2...
Member: Sean C. Butler, Ph.D.

DocuSigned by:
68AB406F2478433...
Member: Dustin P. Patterson, Ph.D.

DocuSigned by:
Tanya Sklyoko
4401B5CA640A497...
Chair, Department of Chemistry and Biochemistry

DocuSigned by:
Neil Gray
A1D7A503B8334DF...
Dean, College of Arts and Sciences

ACKNOWLEDGMENT

I am grateful to God for giving me the desire and opportunity to get into science and pursue a degree in chemistry. He gave me a strong desire to learn, which helped give me the motivation to carry on throughout my studies.

I would like to thank Dr. Jiyong Lee for guiding my research and helping me learn more about chemistry. The research I conducted with him has given me a greater understanding of techniques and instruments that I would not have gotten otherwise. I also want to thank Dr. Dustin P. Patterson, and Dr. Sean C. Butler for answering any questions I had, as well as the other faculty at the department of chemistry and biochemistry for their help.

I also want to thank my family for raising and supporting me throughout my life, as well as encouraging me to get a master's degree. Without their support I would not have been able to come this far in my pursuit of knowledge.

Table of Contents

List of Figures

List of Abbreviations

Abs	absorbance
A_{280}	absorbance at 280 nanometers
A_{495}	absorbance at 495 nanometers
Aldox	Aldoxorubicin
Alloc	allyloxycarbonyl
BSA	bovine serum albumin
BCS	breast cancer cell
BCSC	breast cancer stem cell
Boc	tert-butyloxycarbonyl
CSC	cancer stem cell
cm	centimeter(s)
CAA	chloroacetic acid
° C	degrees celsius
di	deionized
DNA	deoxyribonucleic acid
d. nm	diameter in nanometers
DIC	diisopropylcarbodiimide
DIPEA	N,N-diisopropylethylamine
DMF	N,N'-dimethylforamide
DMSO	dimethyl sulfoxide
dd	double distilled
Dox	doxorubicin

DLS	dynamic light scattering
EDTA	ethylenediaminetetraacetic acid
EMCH	N-ε-maleimidocaproic acid hydrazide
Fmoc	fluorenylmethoxycarbonyl protecting group
HPLC	high-performance liquid chromatography
h	hour(s)
HBTU	hexafluorophosphatebenzotriazoltetramethyluronium
HOBt	hydroxybenzotriazole
kDa	kilodalton(s)
LC	liquid chromatography
LC-MS	liquid chromatography-mass spectrometry
MBHA	methylbenzhydryl amine
miRNA	micro ribonucleic acid
µg	microgram(s)
µL	microliter(s)
µm	micrometer(s)
µM	micromolar
mg	milligram(s)
mL	milliliter(s)
mm	millimeter(s)
mM	millimolar
M	molar
MWCO	molecular weight cutoff

nm	nanometer(s)
NMP	N-Methylpyrrolidone
%V	percent volume
PBS	phosphate buffered saline
PDI	polydispersity
PEG	polyethylene glycol
PVDF	polyvinylidene difluoride
RT	room temperature
rpm	rotations per minute
shRNA	short hairpin ribonucleic acid
TFA	trifluoroacetic acid
TIS	triisopropylsilane
TNBC	triple negative breast cancer
TBS	tris buffered saline
TBST	tris buffered saline with polysorbate 20
Tris	Tris(hydroxymethyl)aminomethane
UV	ultraviolet
VLP	virus like particle
V	volts
WT	wild type

Amino Acids

E (glu)	glutamic acid
Q (Gln)	glutamine
G (gly)	glycine
L (leu)	leucine
K (Lys)	lysine
P (pro)	proline
T (thr)	threonine

Abstract

USING VIRUS LIKE PARTICLE CONJUGATES OF SYNTHETIC TARGETING COMPOUNDS TO DELIVER CHEMOTHERAPEUTIC DRUGS TO CANCER STEM CELLS

Austen Kerzee

Thesis Chair: Jiyong Lee, Ph.D.

The University of Texas at Tyler
March 2024

Cancer stem cells are a type of cell that have the properties of both cancer cells and stem cells. They can differentiate into other types of cancer cells, are resistant to conventional chemotherapeutics, and seem to contribute greatly to the metastasis and recurrence of cancer. Due to these properties, eliminating cancer stem cells would be greatly beneficial in the treatment of cancer. While there have been approved therapeutic methods for the removal of a few of the cancer stem cells types, treatment for most types of cancer stem cells are still in the experimental phase and have yet to be used in a clinical setting.

This paper discusses the synthesis of the virus like particle conjugates of a breast cancer stem cell targeting compound that binds preferentially to breast cancer stem cells. Once in the cell, it is designed to release a chemotherapeutic drug to initiate apoptosis. This research can potentially be used in the future to help treat breast cancer, and be used as a model for treating other types of cancer as well.

Chapter 1

Overview of Cancer Stem Cells and the State of Research

1.1 Cancer Stem Cell Overview

Cancer stem cells (CSCs) are a type of cancer cell that contribute greatly to the growth and spread of tumors.[1,2,3,4,5] CSCs show self-renewal, differentiation, tumorigenicity when transplanted, and seem to contribute to cancer metastasis.[1,2,3,4,5] They have also been shown to be resistant to conventional chemotherapy treatment.[1,2,3,4,5] CSCs have been shown to have a different expression of cell surface markers compared to other types of cells, such as a $CD24^{-}$ /$CD44^{+}$ phenotype in breast cancer stem cells (BCSCs).[1,2,4,5] These differences can be used to specifically target CSCs to reduce the growth, metastasis, and resistance of tumors. The remaining cancer cells in the tumors can then be treated in a more traditional way.

1.2 The State of Research

There have been several studies showing specific targeting of different kinds of CSCs,[2,3,5] such as targeting CD44 with a monoclonal antibody and reducing the levels of acute myeloid leukemia,[6] using curcumin which inhibits a signaling pathway in liver CSCs,[7] and a few FDA approved drugs such as Vismodegib which is a hedgehog pathway inhibitor that targets basal-cell carcinoma CSCs.[8]

However, there are currently no treatments in clinical use that specifically target BCSCs, though there are many methods of treatment being studied. Here, several of these methods are outlined.

1.2.1 Treatment of Breast Cancer Stem Cells with Salinomycin

One example investigated a compound screening against modified human mammary epithelial (HMLE) breast cancer cells, and discovered that the compound salinomycin showed selective toxicity toward BCSCs.[9]

First modified HMLER cells were prepared by using short hairpin RNA (shRNA)-mediated inhibition of the human CDH1 gene, which encodes E-cadherin, to cause the HMLER cells to undergo an epithelial-mesenchymal transition, and acquire a mesenchymal phenotype.[9] The modified HMLER cell line was then tested for CSC like properties.[9] First, fluorescence-activated cell sorting was used to show that the percentage of cells with the $CD24^-/CD44^+$ phenotype was greater in the modified HMLER cell line when compared to the control HMLER cell line (Figure 1.1 A).[9] Next it was shown that the modified HMLER cell line had a greater ability to form tumorspheres in suspension cultures (Figure 1.1 B) and in mice (Figure 1.1 C) than the control cell line.[9] Lastly it was shown that the modified HMLER cell line possessed a greater resistance to both paclitaxel and doxorubicin than the control cell line (Figure 1.1 D).[9]

HMLE cells, which are not tumorigenic, were then modified the same way as the modified HMLER cells.[9] In comparison to control HMLE cells, the modified HMLE cells also showed an increase in percentage of $CD24^-/CD44^+$ phenotype cells (Figure 1.1 A), and a resistance to several common chemotherapeutic drugs (Figure 1.1 E).[9]

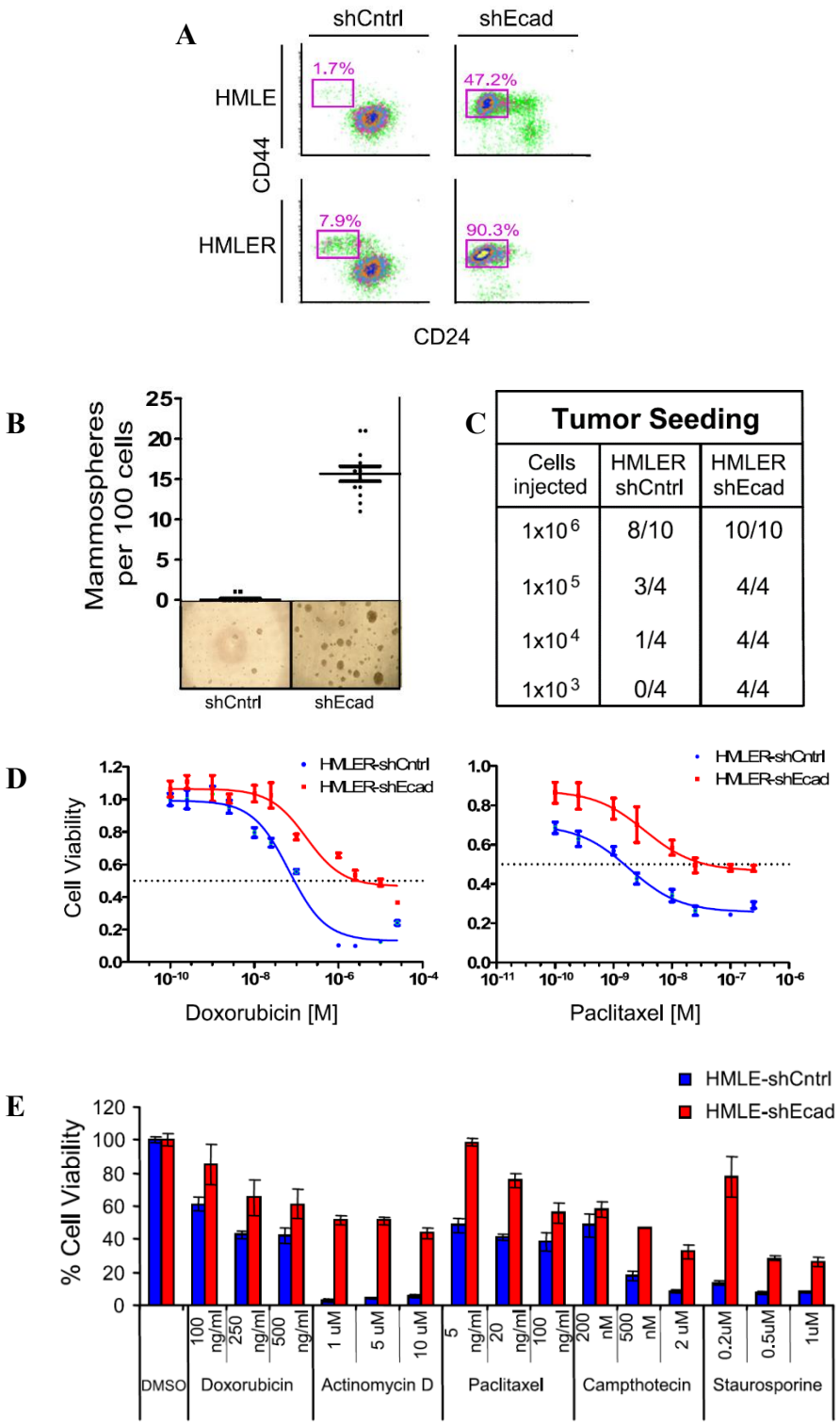

Figure 1.1. A: Fluorescence-activated cell sorting of HMLER and HMLE modified (shEcad) and unmodified (shCntrl) cell populations. The percentage of cells with the $CD24^{-}/CD44^{+}$ phenotype is shown in pink. B: The mammosphere forming capability of the modified (shEcad) and unmodified (shCntrl) HMLER cell lines.

Figure 1.1 (Continued)

C: Graph showing the ability of the modified (shEcad) and unmodified (shCntrl) HMLER cell lines to form tumors when injected into mice. The numbers are given in injections given/ tumors formed. D: Graph comparing the resistance of the modified (HMLER-shEcad) and unmodified (HMLER-shCntrl) HMLER cell lines to the chemotherapeutic drugs Doxorubicin and paclitaxel. E: Graph comparing the resistance of the modified (HMLE-shEcad) and unmodified (HMLE-shCntrl) HMLE cell lines to common chemotherapeutic drugs at varying concentrations, using DMSO as a control.

For chemical screening, modified and control HMLE cells were treated with the test compounds, and checked for viability after three days.[9] Out of 16000 compounds, only 10% reduced the viability of the modified HMLE cells, and only 2% did not also reduce the viability of the control HMLE cells.[9] Only four of these compounds showed selective toxicity toward the modified HMLE cells (Figure 1.2 A), and out of those only the compound salinomycin showed a high amount of selective toxicity toward modified HMLER cells as well (Figure 1.2 B).[9]

The ability of salinomycin to reduce the percentage of $CD24^-/ CD44^+$ cells in the modified HMLER cells was compared to the chemotherapeutic drug paclitaxel.[9] It was found that while the percentage of $CD24^-/ CD44^+$ cells was reduced after treatment with salinomycin in comparison to DMSO, the number of $CD24^-/ CD44^+$ cells increased after treatment with paclitaxel (Figure 1.3 A).[9] Treatment of unmodified HMLER cell lines, which naturally contain a high number of CSCs, with salinomycin also showed a decrease in the percentage of $CD24^-/ CD44^+$ cells (Figure 1.3 A).[9] Treatment with salinomycin also greatly reduced the ability of HMLER cells to form tumorspheres when compared with paclitaxel, and DMSO (Figure 1.3 B).[9]

A later study on the mechanism of action for salinomycin seemed to show that it accumulates and isolates iron in lysosomes, causing the degradation of ferritin in lysosomes and the accumulation of even more iron.[10] The increased iron levels led to the iron mediated production of reactive oxygen species, which then causes lysosomal membrane permeabilization,

and eventually initiation of apoptosis.[10] Although it shows promise, treatment of BCSC with salinomycin is still in the research phase.

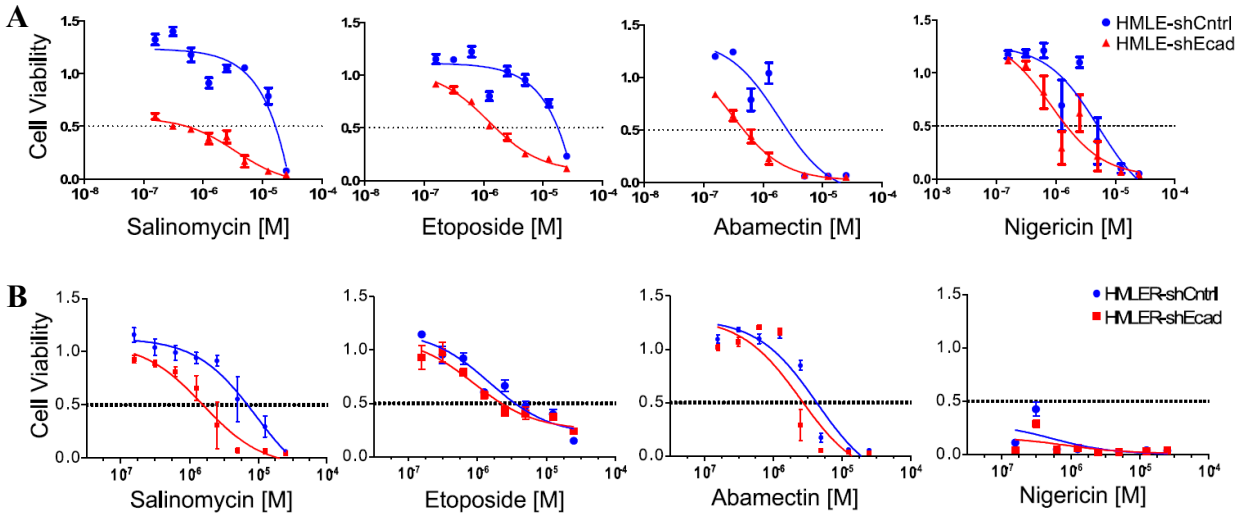

Figure 1.2. A: Graph showing the selective toxicity of four of the four chosen compounds against modified (HMLE-shEcad) and unmodified (HMLE-shCntrl) HMLE cell lines with increasing dosage. B: Graph showing the selective toxicity of four of the four chosen compounds against modified (HMLER-shEcad) and unmodified (HMLER-shCntrl) HMLER cell lines with increasing dosage.

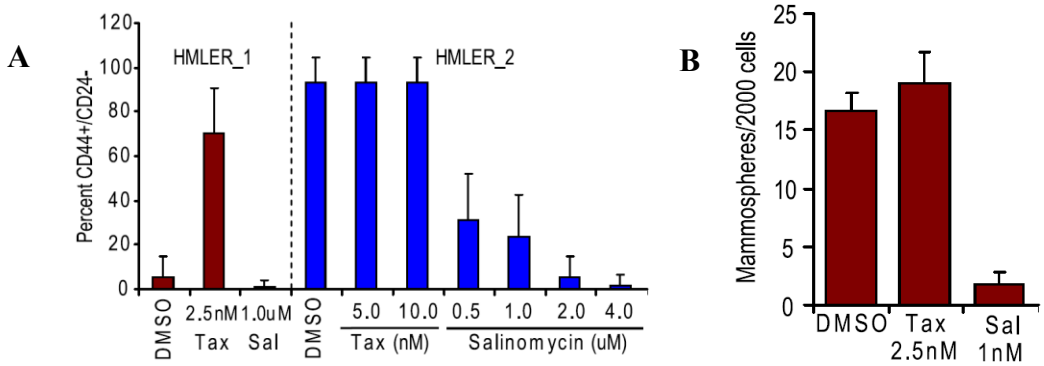

Figure 1.3. A: Graph showing the percentage of $CD24^{-}/CD44^{+}$ cells in modified (HMLER_1) and unmodified (HMLER_2) HMLER cell lines after treatment with salinomycin, paclitaxel, and DMSO. B: Graph showing the ability of unmodified HMLER cells to form mammospheres after treatment with salinomycin, paclitaxel, and DMSO.

1.2.2 Treatment of Breast Cancer Stem Cells with Phytochemicals

A second example looked at the selective binding of several phytochemicals for MCF-7 breast cancer stem cells over regular MCF-7 breast cancer cells, and found that three of the phytochemicals, 6-Gingerol, 6-Shogol, and Pterostilbene, showed selective toxicity toward BCSCs.[11]

MCF-7 cells were suspended in PBS with 1% FBS and 1% penicillin / streptomycin, fluorochrome conjugated monoclonal antibodies against human CD44 (FITC) and CD24 (PE) were added, and the solution was incubated.[11] A FACSAria Cell Sorter unit was used to analyze the cells, with the $CD24^{-/low}/CD44^{+}$ phenotype being used to identify and isolate BCSCs.[11] The purity and viability of the cells was observed to be above 98% using trypan blue dye exclusion.[11]

Out of the phytochemicals selected for this study, 6-Gingerol (Figure 1.4 A), 6-Shogol (Figure 1.4 B), and Pterostilbene (Figure 1.4 C) all showed a greater toxicity toward the $CD24^{-}/CD44^{+}$ phenotype MCF-7 cells (Figure 1.5 A) than toward regular MCF-7 cells (Figure 1.5 B).[11] 6-Shogol and Pterostilbene also showed an ability to induce membrane injury in the BCSC mammospheres, while 6-Gingerol did not (Figure 1.6).[11] Treatment of the BCSCs with 6-Shogol and Pterostilbene in combination with paclitaxel was also conducted.[11] This showed that treatment with either 6-Shogol or Pterostilbene in combination with paclitaxel reduced the viability of BCSCs more than paclitaxel alone (Figure 1.7).[11]

The mechanism of action for 6-Shogol and Pterostilbene is believed to be that they cause the phosphorylation and degradation of the β-catenin protein, thus reducing CD44 activity, and causing a loss of stemness in BCSCs.[11] Just like with salinomycin however, treatment of BCSC with these phytochemicals is still in the research phase.

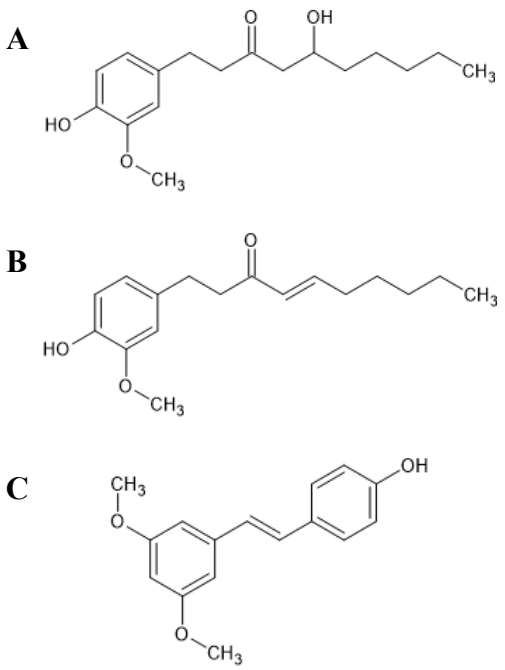

Figure 1.4. The structures of the compounds showing selective toxicity; 6-Gingerol (A), 6-Shogol (B), and Pterostilbene (C).

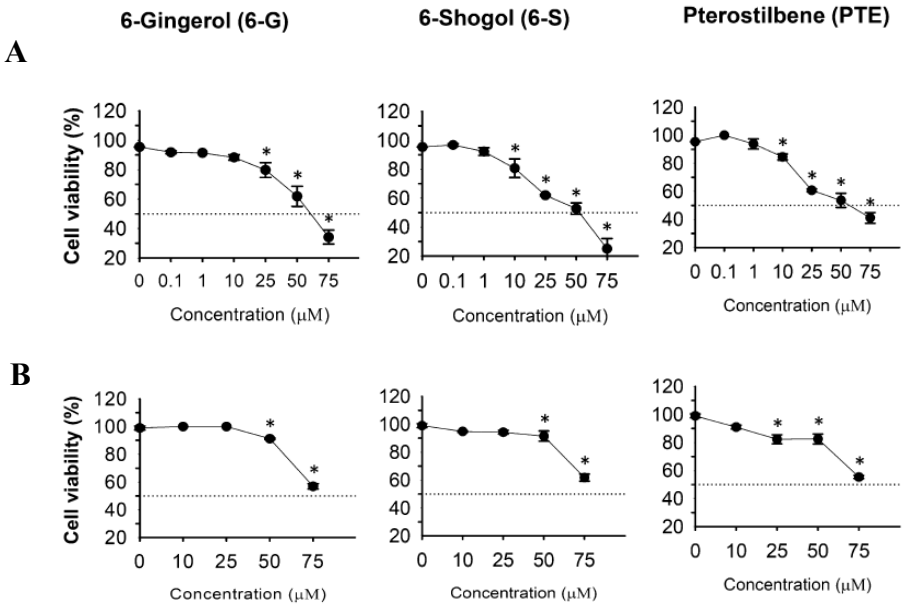

Figure 1.5. Chart showing the viability of $CD44^{+}/CD24^{-}$ MCF-7 cells (A) and regular MCF-7 cells (B) after treatment with 6-Gingerol, 6-Shogol, and Pterostilbene for 72 hours.

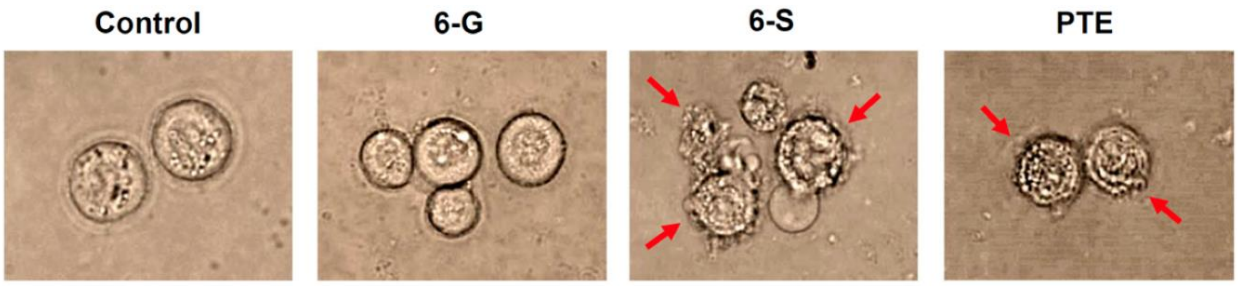

Figure 1.6. Figure showing the ability of 6-Gingerol (6-G), 6-Shogol (6-S), and Pterostilbene (PTE) to induce membrane injury in BCSC mammospheres. The red arrows show observed membrane damage.

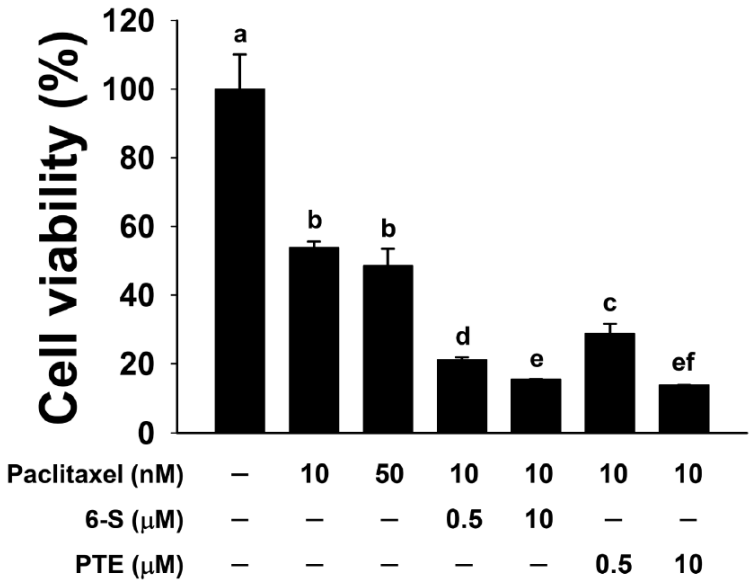

Figure 1.7. Graph showing percent cell viability of BCSCs after treatment with different combinations and concentrations of Paclitaxel, 6-Shogol (6-S), and Pterostilbene (PTE).

1.2.3 Treatment of Breast Cancer Stem Cells with an Osmium(VI) Nitrido Complex

A third example looked at the anti-cancer stem cell activity of several osmium nitrido and platinum complexes, and found that an osmium(VI) nitrido complex showed selective toxicity toward HMLER BCSCs.[12]

Following a previously reported method, HMLER breast cancer cells were treated with paclitaxel for four days, leading to a HMLER cell population with more than 30% of cells displaying a $CD44^{high}$ phenotype.[12]

First the IC_{50} values against regular and $CD44^{high}$ HMLER cells were determined for several osmium nitride and platinum complexes, several known anti-cancer drugs like cisplatin, and two compounds known to display selective toxicity against CSCs, salinomycin and abamectin.[12] Only one of the osmium(VI) nitride complexes (Figure 1.8), along with salinomycin and abamectin, showed selective toxicity toward the $CD44^{high}$ HMLER cell line over the regular HMLER cell line (Figure 1.9).[12] The osmium(VI) nitride complex was then compared to other drugs in their ability to decrease the number of mammospheres in the $CD44^{high}$ HMLER cell line after treatment at their IC_{30} values for five days.[12] The osmium(VI) nitride complex and salinomycin showed the largest decreases in the number of mammospheres, with the osmium(VI) nitride complex showing a 38% decrease (Figure 1.10).[12]

The mechanism of action for the osmium(VI) nitride complex was determined to be that it causes both endoplasmic reticulum stress and DNA damage, leading to apoptosis of the cell.[12] Just like the other two treatments however, treatment of BCSC with this osmium(VI) nitride complex is still in the research phase.

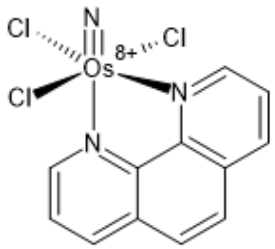

Figure 1.8. The structure of the BCSC selective Osmium(VI) Nitrido Complex.

compound	HMLER IC_{50} (μM)	$HMLER^{tax}$ IC_{50} (μM)	selectivity for $HMLER^{tax}$ [a]
1	11.20 ± 0.48	4.91 ± 0.86	2.31
2	14.58 ± 0.20	16.06 ± 4.12	0.91
3	82.80 ± 18.43	53.99 ± 2.45	1.53
salinomycin	0.49 ± 0.26	0.058 ± 0.01	8.45
abamectin	1.45 ± 0.18	0.64 ± 0.06	2.26
cisplatin	1.95 ± 0.40	2.06 ± 0.67	0.95
carboplatin	17.84 ± 0.58	18.19 ± 0.80	0.98
oxaliplatin	15.04 ± 0.41	26.95 ± 4.42	0.55
satraplatin	1.22 ± 0.06	2.87 ± 0.23	0.43
Pt(IV)-C2	39.09 ± 9.82	40.64 ± 9.91	0.96
Pt(IV)-C16	0.0254 ± 0.0016	0.1131 ± 0.0197	0.22

Figure 1.9. A chart showing the IC_{50} and selectivity values of the different testing compounds against cells from regular (HMLER) and $CD44^{high}$ ($HMLER^{tax}$) HMLER cell lines. Only one of the osmium(VI) nitrido complexes (1) showed highly selective toxicity toward $CD44^{high}$ ($HMLER^{tax}$) HMLER cells, while the other two (2 and 3) showed little or no selectivity.

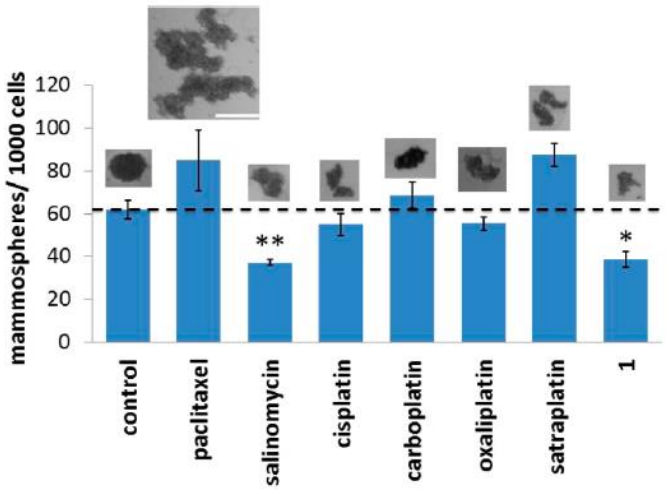

Figure 1.10. Mammosphere formation of $CD44^{high}$ HMLER cells after treatment with the osmium(VI) nitrido complex (1) and several other known compounds, all at their IC_{30} values for five days.

Chapter 2

Using Virus Like Particle Conjugates of Synthetic Targeting Compounds to Deliver Chemotherapeutic Drugs to Breast Cancer Stem Cells

2.1 The BCSC Targeting Compound

A compound was previously discovered that showed preferential binding toward breast cancer stem cells containing the $CD24^-/CD44^+/ALDH^+$ phenotype.[13] This compound was found via a cell-binding screening of a chemical library, and consists of eight peptoid residues (Figure 2.1).[13] Cell lines from MCF-7 and MDA-MB-231 were used to show preferential binding to BCSCs because other studies had suggested these cell lines contained BCSC populations with the $CD24^-/CD44^+$ phenotype.[14,15] The compound was bound to tentagel beads and incubated with MCF-7 and MDA-MB-231 cell lines separately to isolate suspected BCSCs from the general BCC population.[13]

The cells that bound to the binding compound were then tested to determine if they were BCSCs. Increased ALDH enzyme activity has been shown to be associated with CSC populations.[16,17,18] The binding, non-binding, and wild type cells from MCF-7 (Figure 2.2 A) and MDA-MB-231 (Figure 2.2 B) were tested for increased ALDH activity using Aldefluor staining, showing that the binding populations had an increased amount of ALDH activity compared to the non-binding and wild type cell populations.[13] Then expression levels of the stemness-associated transcription factors c-Myc, Klf4, Sox2, and Nanog were compared for the binding, non-binding, and wild type cell populations of MCF-7 using western blot, showing an increase expression of all of the transcription factors for the binding cell population (Figure 2.2 C).[13] The same stemness-associated transcription factor levels with the addition of βactin were

compared for the binding, non-binding, and wild type cell populations of MDA-MB-231 using western blot, showing an increased expression of c-Myc, Klf4, and Nanog in the binding cell population (Figure 2.2 D).[13] CSC populations are also known to be tumorigenic,[16] so the binding, non-binding, and wild type MDA-MB-231 populations were tested for tumorigenicity after injection into mice. The binding population showed an increase in tumor volume compared to the wild type population, while the non-binding population showed a decrease in tumor volume compared to the wild type population (Figure 2.3).[13]

Because the compound is simply a selective binding compound, it cannot modulate BCSC activity on its own. A derivative of the compound was made by adding a polyglycine for further conjugation, and a biotin for detection (Figure 2.4). The polyglycine will be conjugated to a virus like particle which will then be used to deliver a chemotherapeutic compound that can modulate BCSC activity.

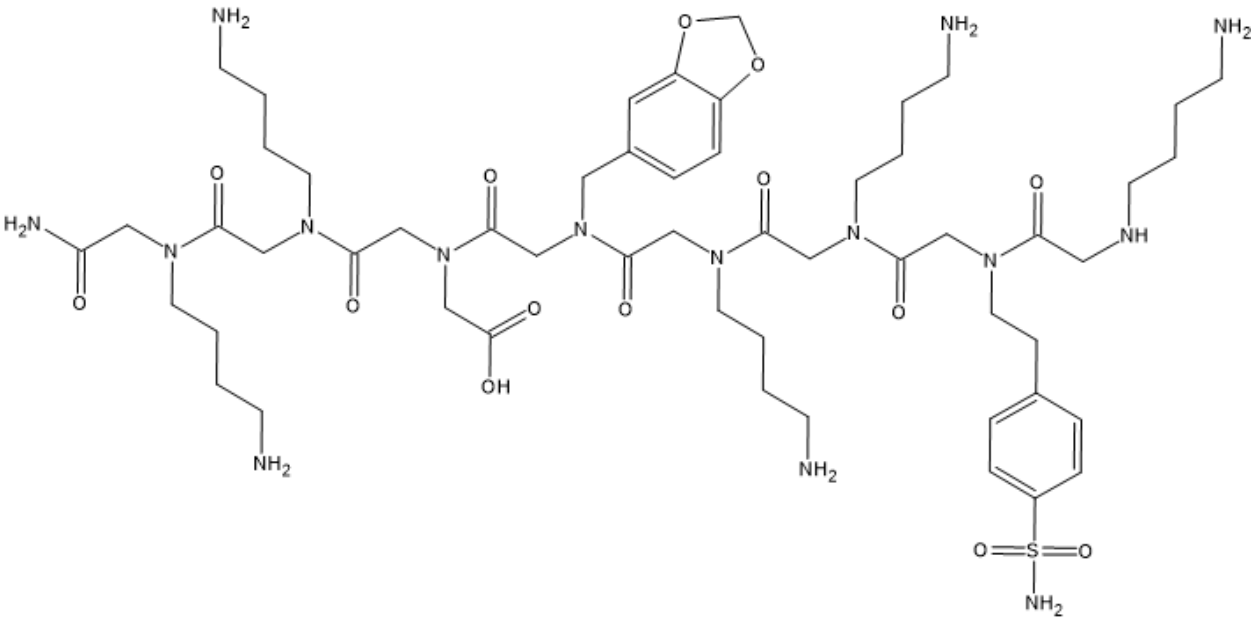

Figure 2.1. The structure of the original BCSC targeting compound CL-1-19-1.

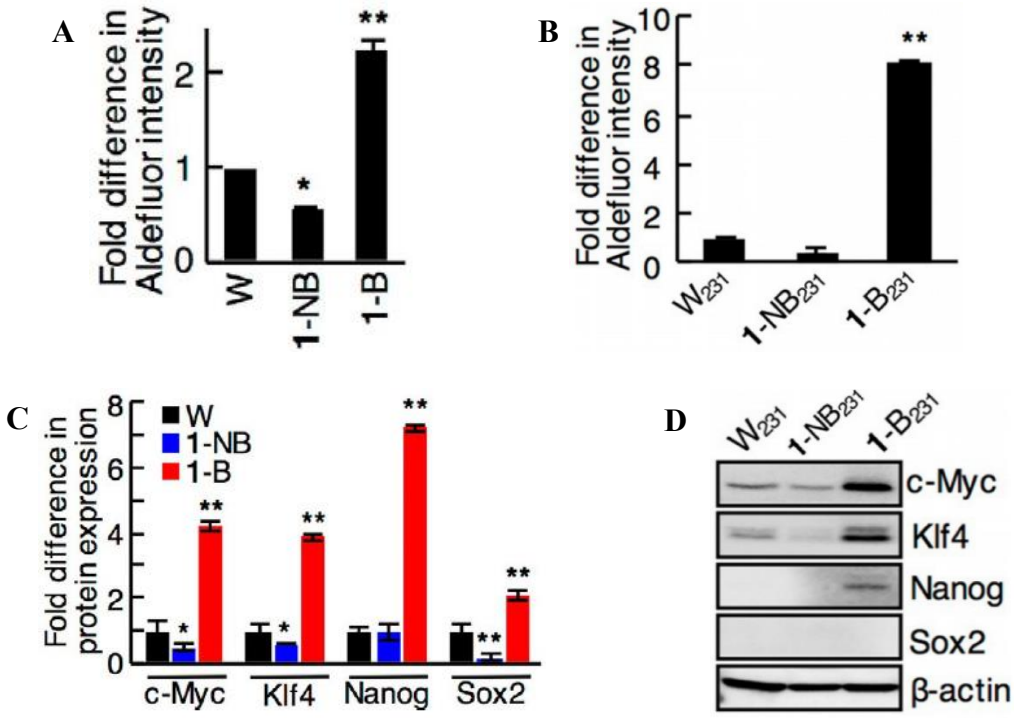

Figure 2.2. Quantitative analysis of Aldefluor staining showing the ALDH activity of WT (W and W_{231}), non-binding (1-NB and 1-NB_{231}), and binding (1-B and 1-B_{231}) cell populations of MCF-7 (A) and MDA-MB-231 (B) cell lines. Western blot analysis showing the expression of stemness-associated transcription factors in WT (W and W_{231}), non-binding (1-NB and 1-NB_{231}), and binding (1-B and 1-B_{231}) cell populations of MCF-7 (C) and MDA-MB-231 (D) cell lines.[13]

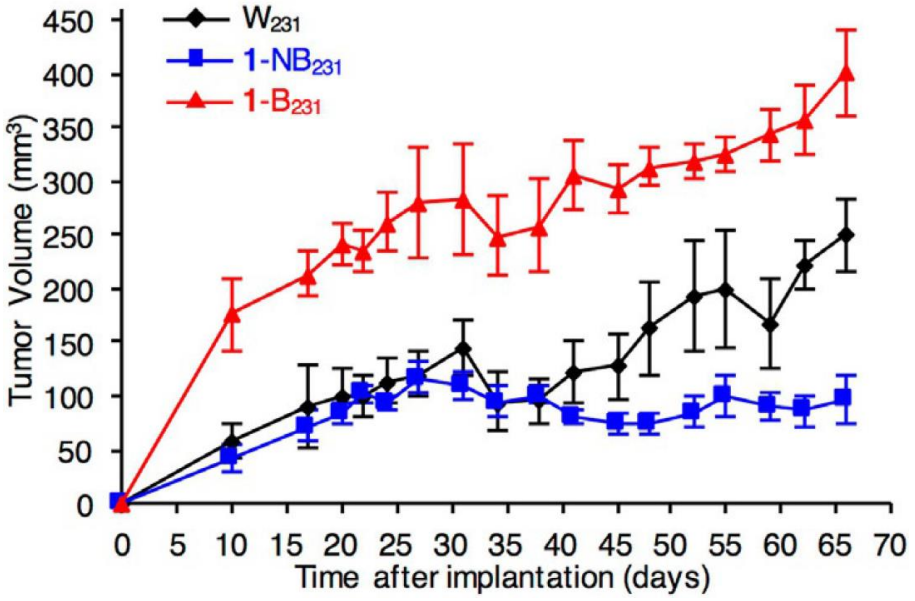

Figure 2.3. Tumoriginicity of the binding (1-B_{231}), non-binding (1-NB_{231}), and wild type (W_{231}) cell populations of the MDA-MB-231 cell line after injection into mice.[13]

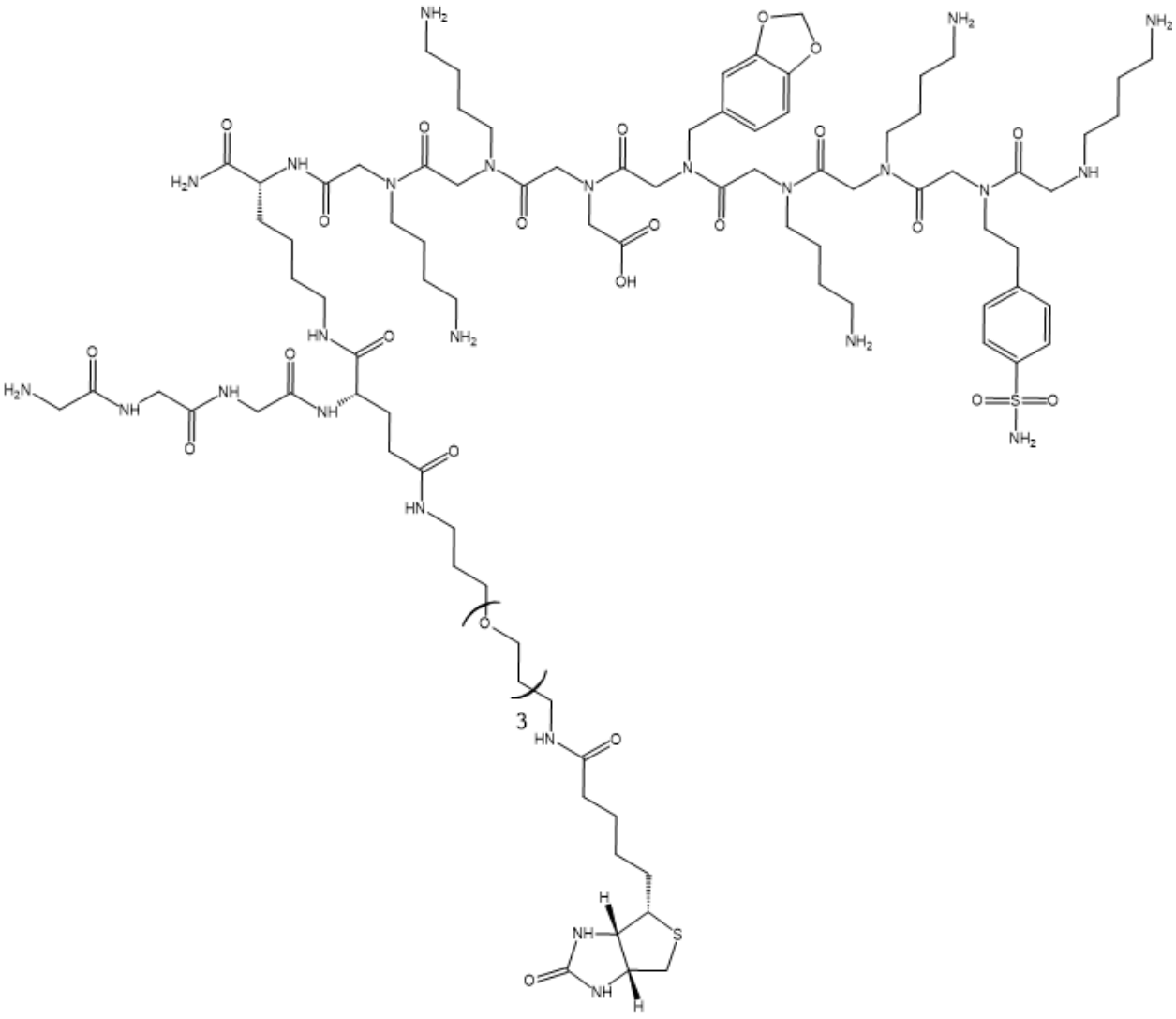

Figure 2.4. A derivative of the BCSC targeting compound with a polyglycine for conjugation to virus like particles with an external LPETG sequence, and a biotin for detection.

2.2 Conjugating to HK-97 VLP

Virus like particles (VLPs) are cage proteins with a diameter usually around 10-100 nm, which allows them to travel through the body and interact with cells easily.[19] VLPs can also be engineered to have different properties than the original, which can give them many uses

including; being platforms for synthesis of immunotherapeutic nanomaterials,[20,21] as drug carriers to deliver drugs to a target,[22] and as chambers for synthesizing nanoparticles.[23]

Some VLPs such as the bacteriophage P22 VLP, have the ability to incorporate a LPETG amino acid sequence to the C-terminus of the coat protein subunits before assembly into the capsid.[19] This C-terminus LPETG sequence along with an N-terminus polyglycine sequence are the peptide recognition sequences used by the sortase enzyme to catalyze peptide bond formation in the presence of calcium.[19] Formation of the peptide bond occurs between the threonine of the LPETG sequence and the N-terminal glycine of the polyglycine sequence.[19] This allows an LPETG modified P22 VLP to conjugate to the polyglycine of a target protein using sortase.[19]

The VLP chosen for conjugation to the BCSC targeting compound was the HK-97 Prohead I VLP from bacteriophage Hong Kong 97. This VLP was chosen because it can be modified for conjugation both internally and externally,[24] has enough space internally to carry a payload,[24] and has little interaction with mammalian cells without external modifications.[25] It consists of 420 copies of the 42 kDa coat protein GP5 that self-assemble to form the Prohead I procapsid used in this study (Figure 2.5).[24,26] It can be transformed further into the Prohead II procapsid in the presence of the GP4 protease, and finally into the Head II capsid in a low pH environment, but these are not used in this study.[24]

The Prohead I HK-97 VLP used in this study was modified by adding the same LPETG amino acid sequence used for the P22 VLP to the C-terminus externally and mutating a serine that was exposed internally into a cysteine.[24] It was also shown that like the P22 VLP, in the presence of sortase the LPETG sequence on the modified Prohead I VLP can be conjugated to the N-terminal polyglycine on a protein, in this case a polyglycine modified green fluorescent protein (GFP).[24] In this study, instead of conjugating the VLP to a polycglycine modified GFP, it

will be conjugated to the N-terminus polyglycine sequence on the BCSC targeting compound (Figures 2.6 and 2.7). The BCSC targeting compound will allow the conjugated VLP to enter BCSCs, but to modulate BCSC activity, an internal payload is also needed.

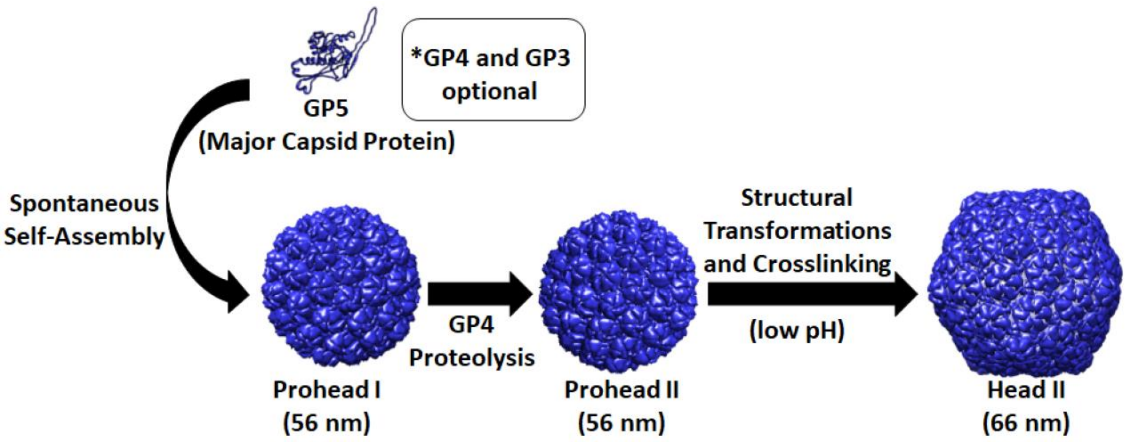

Figure 2.5. The formation of the different capsid structures of the HK-97 VLP using the GP5 protein, GP4 protein, or low pH.[24]

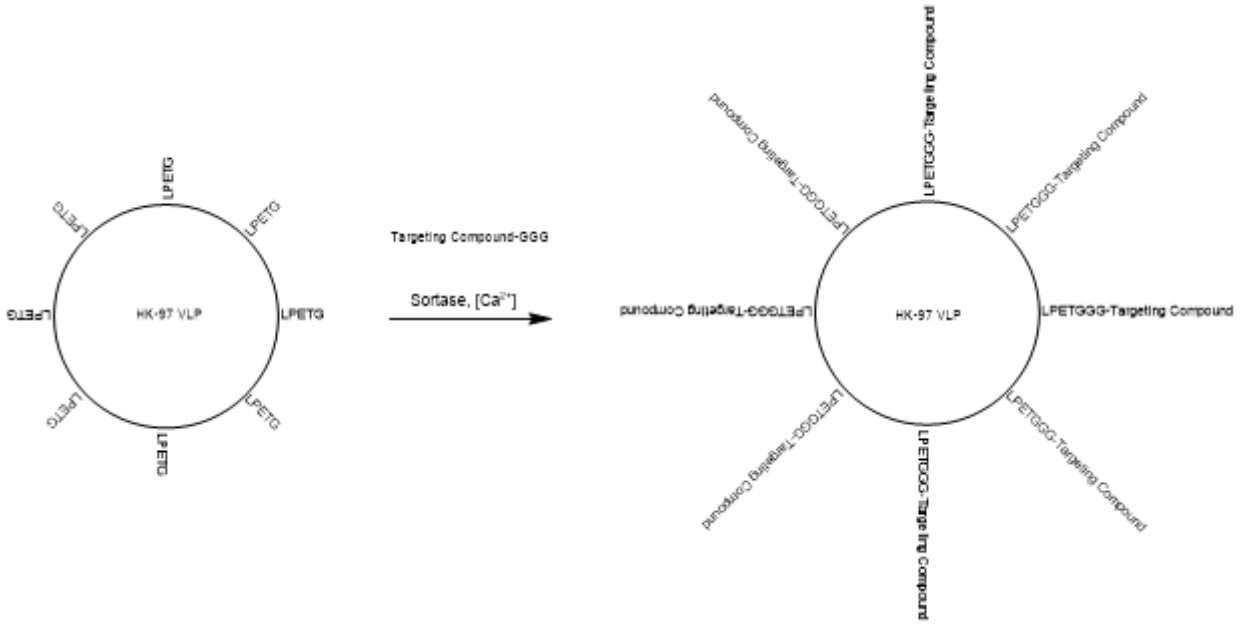

Figure 2.6. Overview of the sortase mediated conjugation reaction of the LPETG sequence on the modified HK-97 VLP with the polyglycine on the BCSC targeting compound derivative.

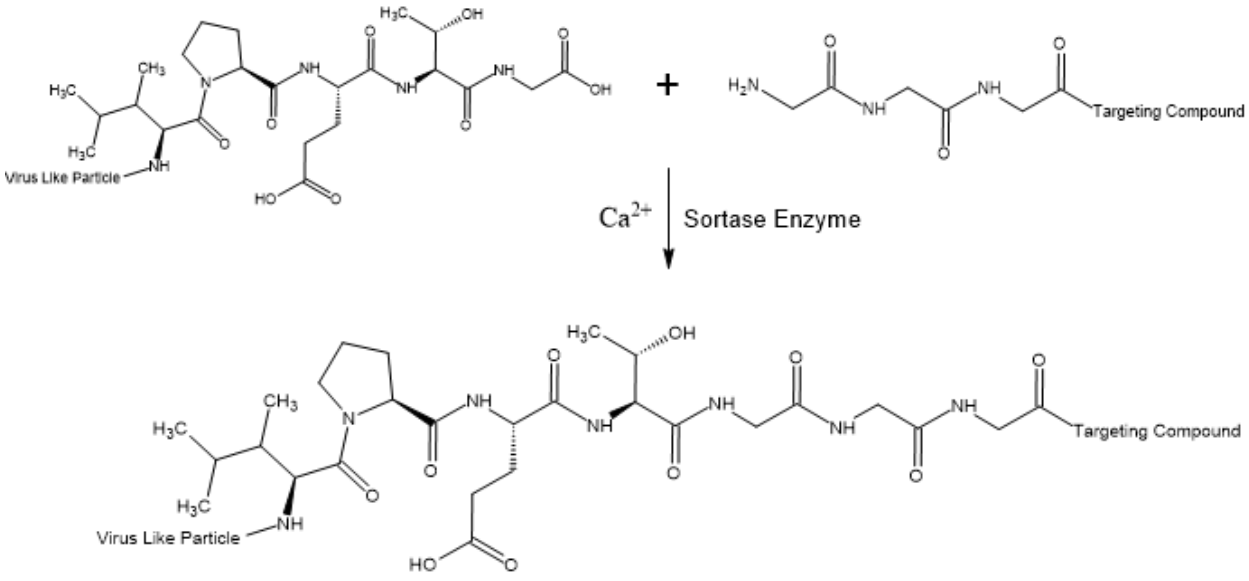

Figure 2.7. The sortase mediated conjugation reaction of the LPETG sequence on the modified HK-97 VLP with the polyglycine on the BCSC targeting compound derivative.

2.3 Encapsulation and Conjugation of a Chemotherapeutic Compound

As mentioned earlier, the HK-97 Prohead I VLP being used also has an internally exposed cysteine that was mutated from a serine.[24] The thiol group on the cystine allows for the conjugation of a payload containing certain functional groups such as a maleimide group to the inside of the VLP.[24] In this study the payload being delivered is the chemotherapeutic drug doxorubicin (Figure 2.8 A). To conjugate Doxorubicin to the VLP however, one of its derivatives called Aldoxorubicin is being used. Aldoxorubicin consists of Doxorubicin bonded to the acid labile compound N-ε-maleimidocapronic acid hydrazide (EMCH) via a hydrazone bond (Figure 2.8 B). Aldoxorubicin is relatively stable at physiological pH (7.4), but undergoes hydrolysis between the Doxorubicin and EMCH in a low pH (5.0) environment (Figure 2.9).[27] The maleimide group in EMCH will be conjugated to the thiol group of the cysteine on the VLP (Figure 2.10).

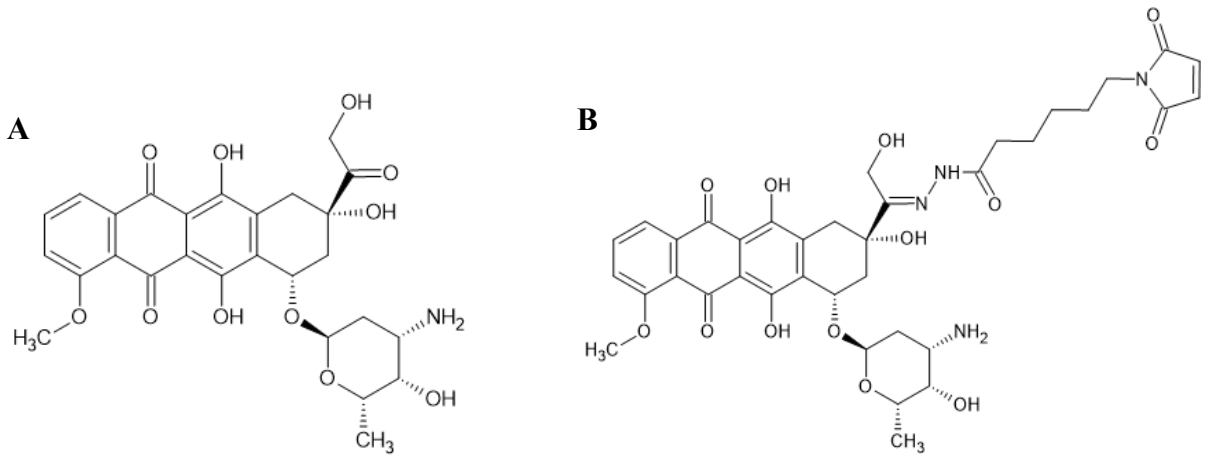

Figure 2.8. The structures of Doxorubicin (A) and Aldoxorubicin (B)

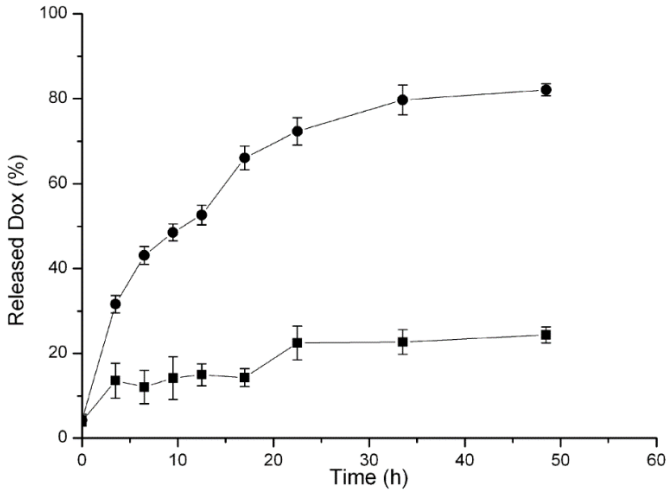

Figure 2.9. Percentage of Doxorubicin released from EMCH in PBS at a pH of 5.0 (top) and 7.4 (Bottom) over time.[27]

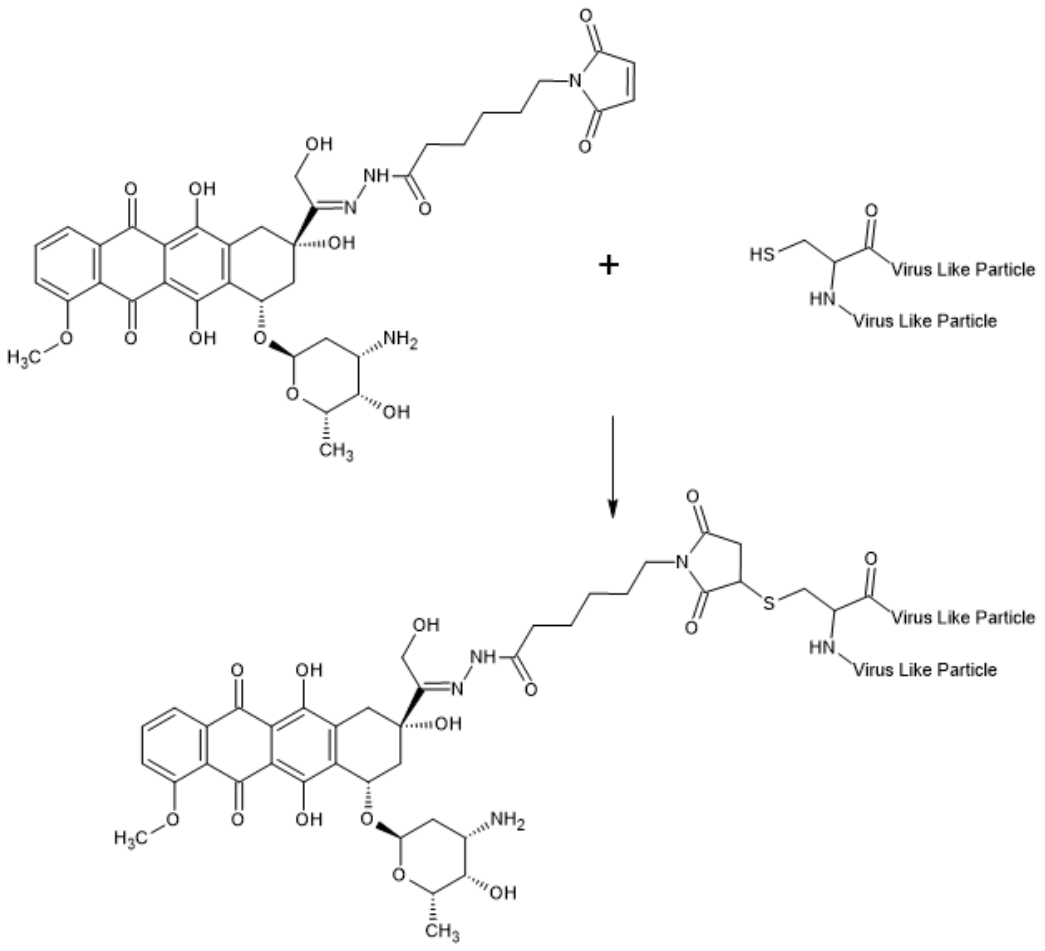

Figure 2.10. The conjugation of the maleimide group on Aldoxorubicin to the thiol of the internal cysteine on the modified HK-97 VLP.

2.4 Release of the Internal Payload into the Cell

After the synthetic binding compound binds to the BCSC, the VLP is expected to be brought into the cell via endocytosis, and eventually will enter a lysosome.[28] The acidic conditions (pH 4.5 – 5.0) in the lysosome should cause hydrolysis of the hydrazone bond in Aldoxorubicin, releasing Doxorubicin (Figure 2.11).[28,27] Once Doxorubicin is in the nucleus, it will intercalate itself into the DNA, disrupting topoisomerase II mediated DNA repair, causing DNA damage, and eventually inducing apoptosis.[29]

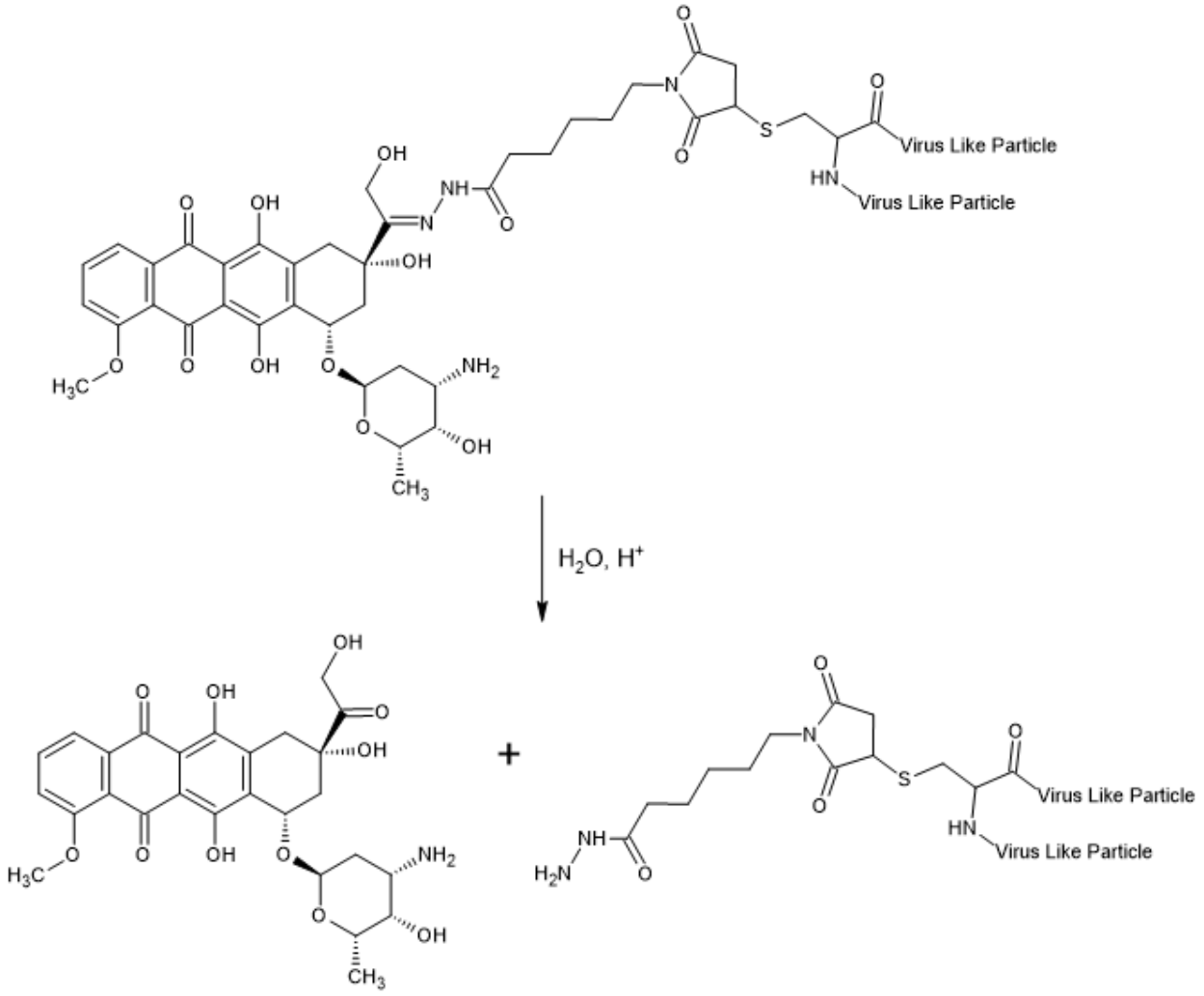

Figure 2.11. The release of Doxorubicin from the conjugated VLP in acidic conditions (pH 5.0) via hydrolysis of the hydrazone group.

Chapter 3

Experimental Results

3.1 Synthesis, Purification, and Characterization of the Breast Cancer Stem Cell Targeting Compound

The BCSC targeting compound was synthesized manually on a Rink Amide MBHA resin. A PEG-biotin group was also added to the targeting compound for detection purposes.

The Fmoc protection group on the resin was removed with piperidine, then Fmoc-Lys(Alloc)-OH was conjugated to the resin in an amination reaction using HOBt, HBTU, and DIPEA as the coupling reagents, and DMF as the solvent (Figure 3.1).

For the first peptoid residue, Boc-diaminobutane was used. Piperidine was once again used to remove the Fmoc group, then CAA was conjugated in an acylation reaction using DIC as the coupling reagent. Boc-diaminobutane was then conjugated to CAA using NMP as the solvent.

The remaining seven peptoid residues all used the same conjugation procedure as the first, minus the Fmoc deprotection step. First CAA was conjugated using DIC as the coupling reagent, then the respective peptoid residues were conjugated using NMP as the solvent. The order of the peptoid residues was; Boc-diaminobutane, H-Gly-OtBu, piperonylamine, Boc-diaminobutane, Boc-diaminobutane, 4-(2-Aminoethyl)benzenesulfonamide, and Boc-diaminobutane. After the final residue, a Boc protection group was added at the end of the peptoid chain to help prevent unwanted binding from occurring (Figure 3.2).

The Alloc protection group from the initial Fmoc-Lys(Alloc)-OH residue was removed by using tetrakis(triphenylphosphine)palladium and phenylsilane as reagents, and dry CH_2Cl_2 as

a solvent. Fmoc-Gln(biotinyl)-PEG-OH was then conjugated to the compound using HOBt, HBTU, and DIPEA as the coupling reagents, and DMF as the solvent (Figure 3.3).

A glycine residue was then added by deprotecting the Fmoc group with piperidine, then conjugating Fmoc-Gly-OH to the compound using HOBt, HBTU, and DIPEA as the coupling reagents, and DMF as the solvent (Figure 3.4). Two more glycine residues were added with the same method to produce a polyglycine chain.

The finished compound was cleaved from the resin using a mixture of TFA, dd water, and TIS (Figure 3.5). It was then dried using nitrogen gas, and stored at -80°C.

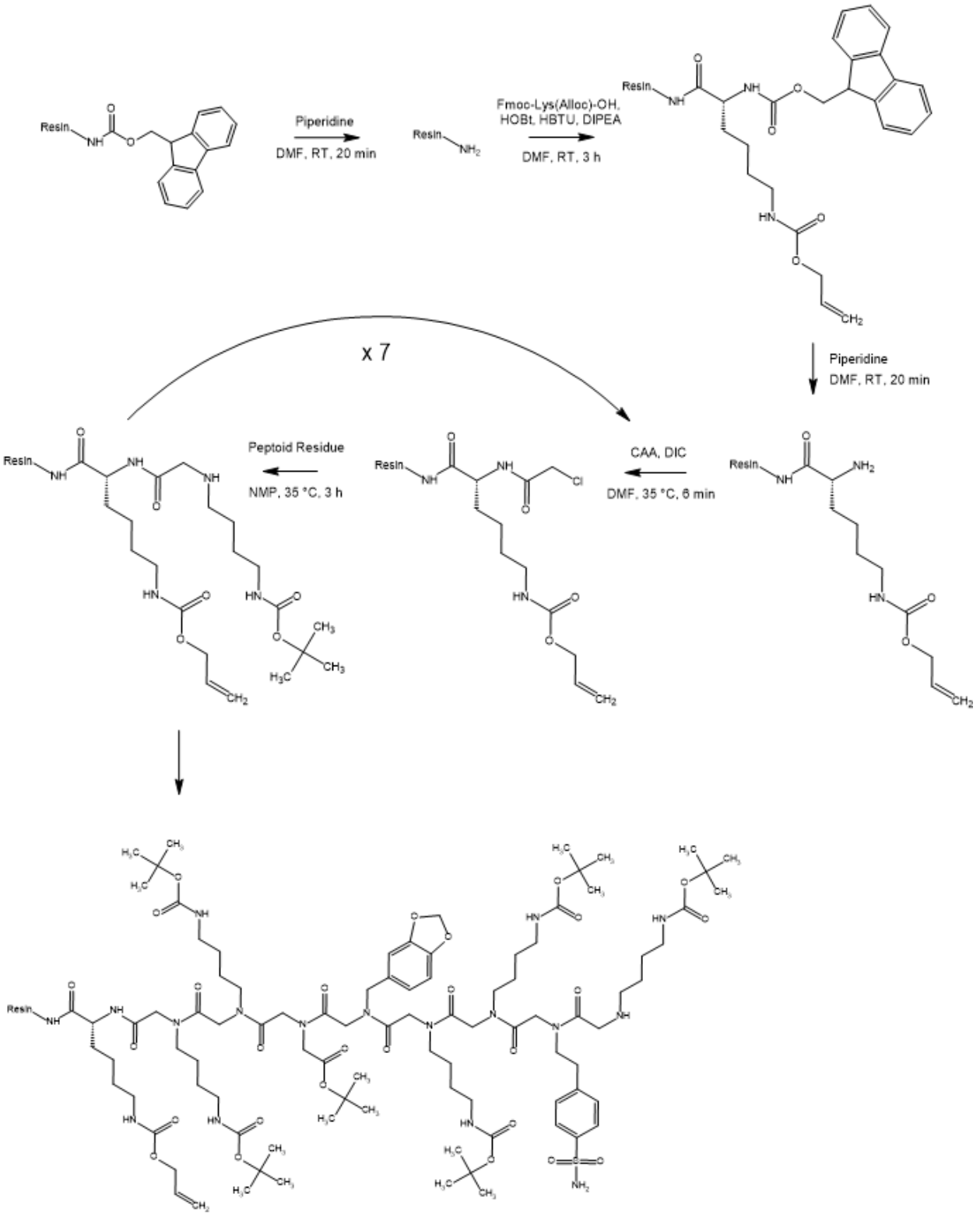

Figure 3.1. Part one of the BCSC targeting compound synthesis.

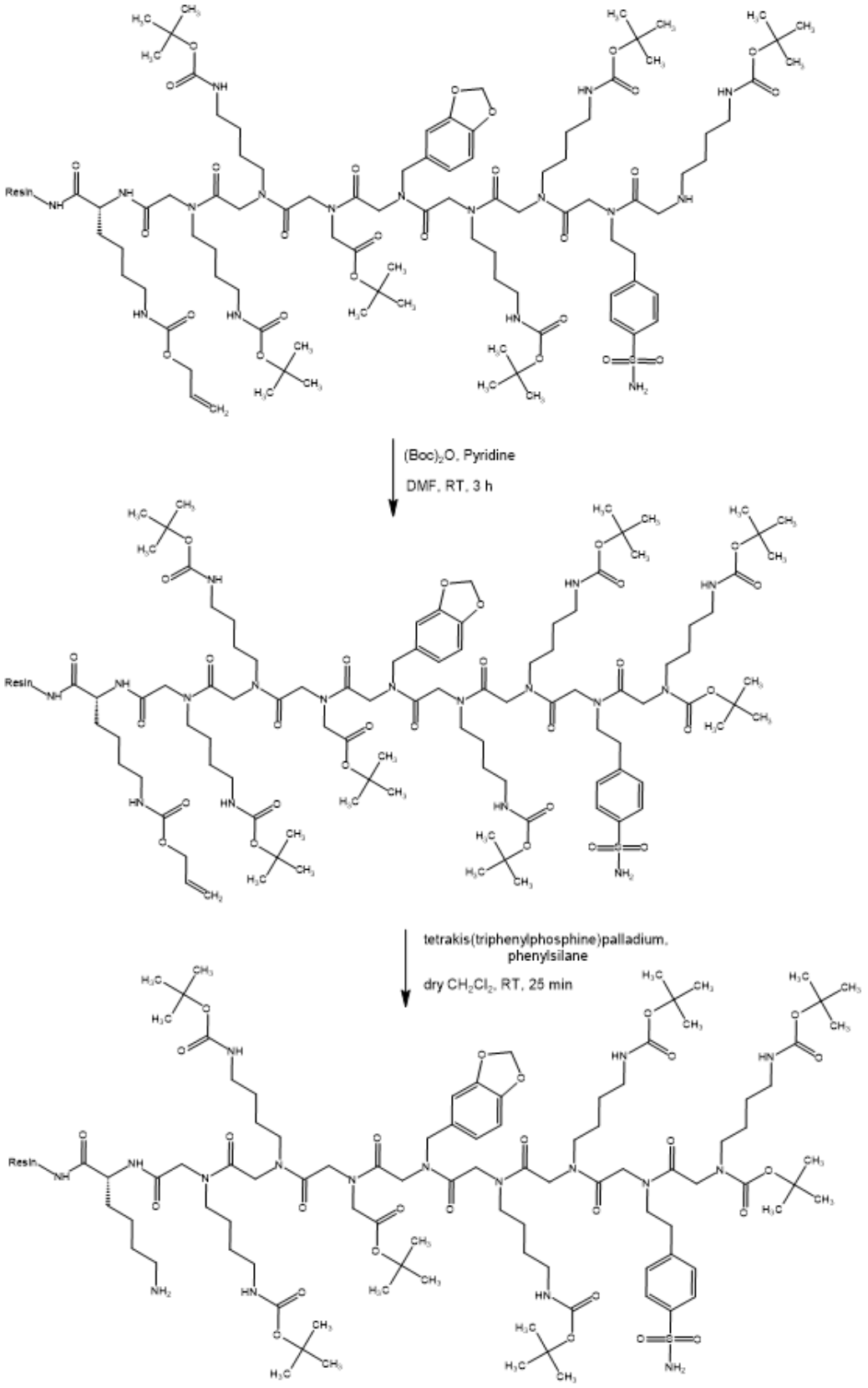

Figure 3.2. Part two of the BCSC targeting compound synthesis.

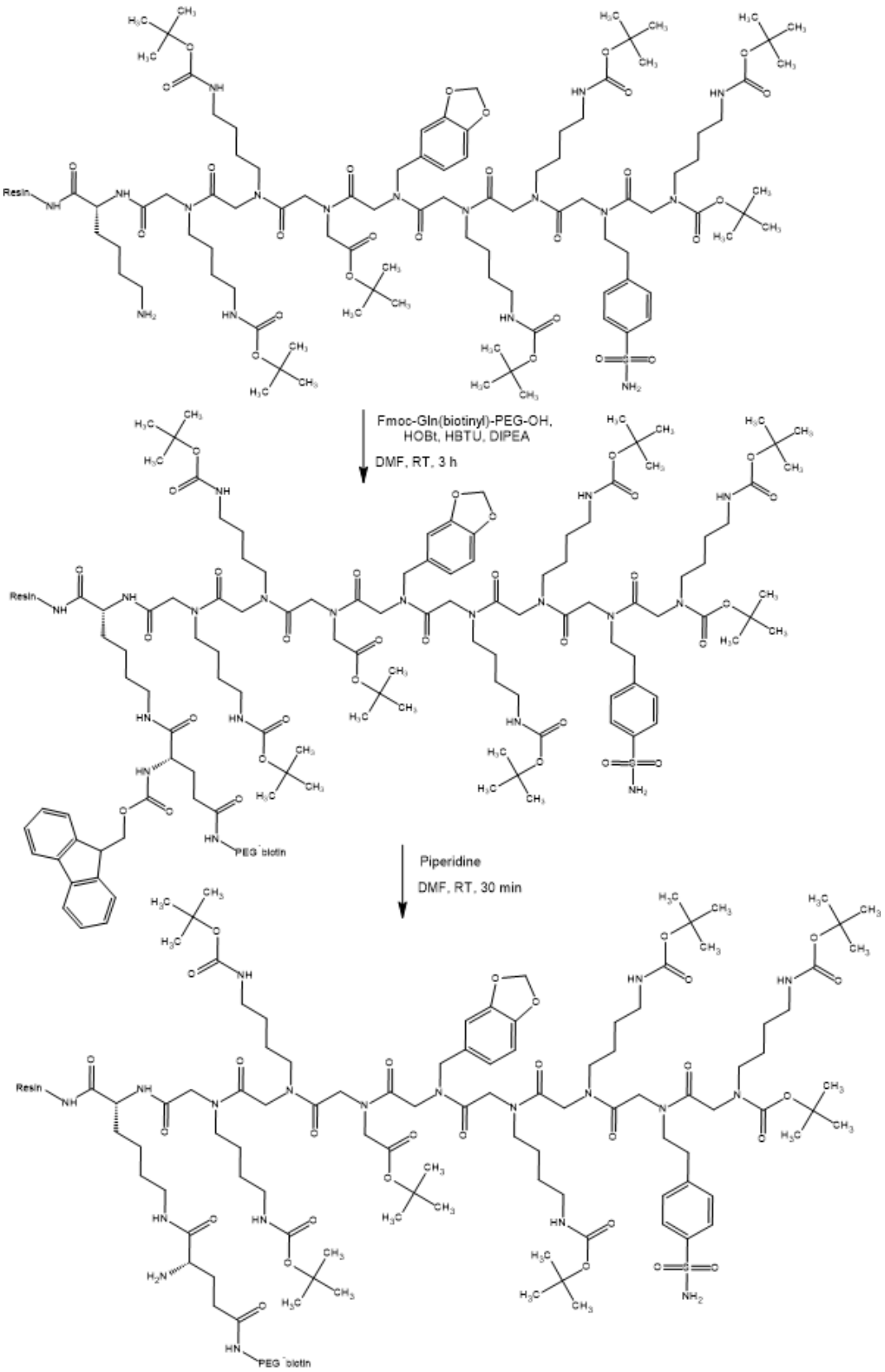

Figure 3.3. Part three of the BCSC targeting compound synthesis.

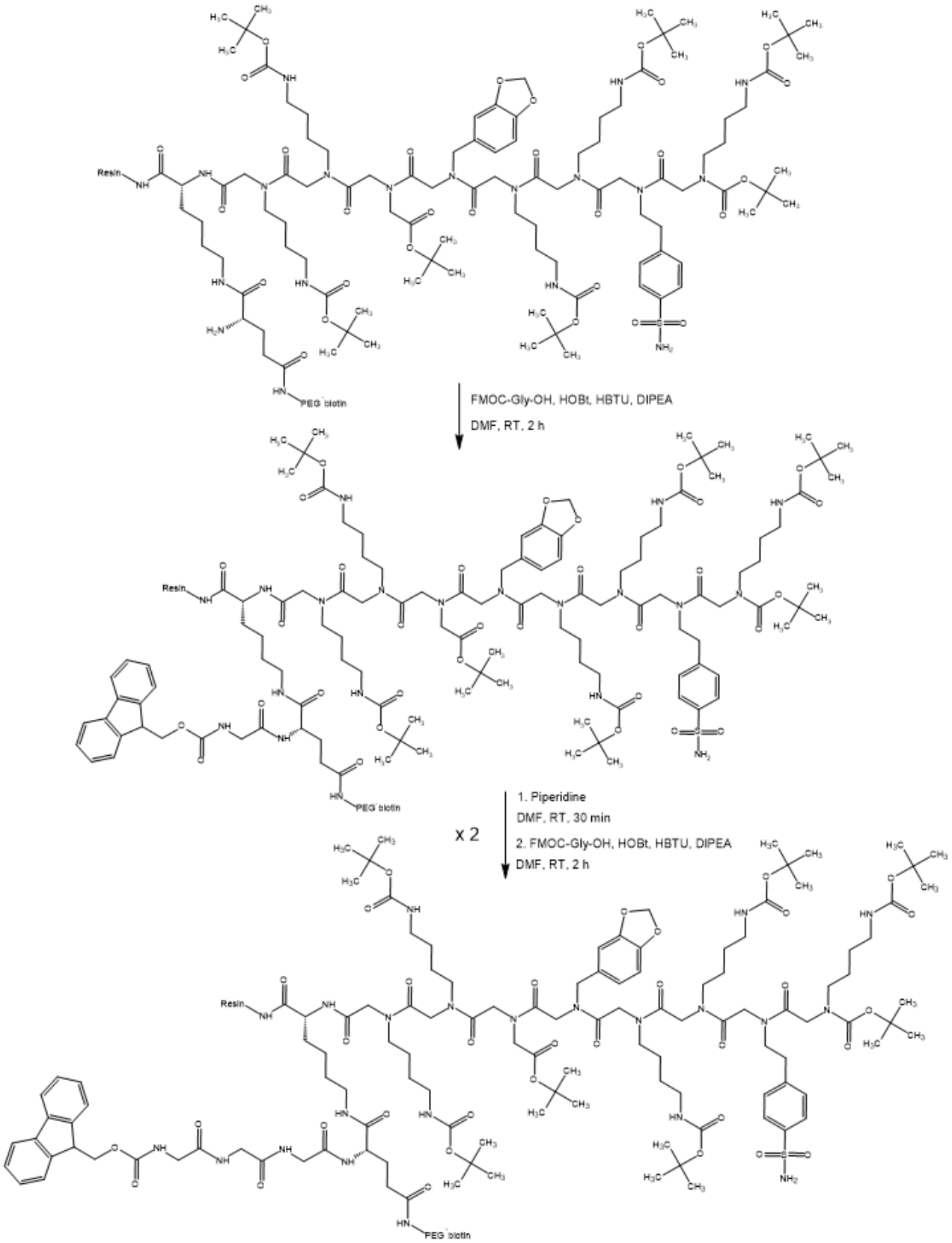

Figure 3.4. Part four of the BCSC targeting compound synthesis.

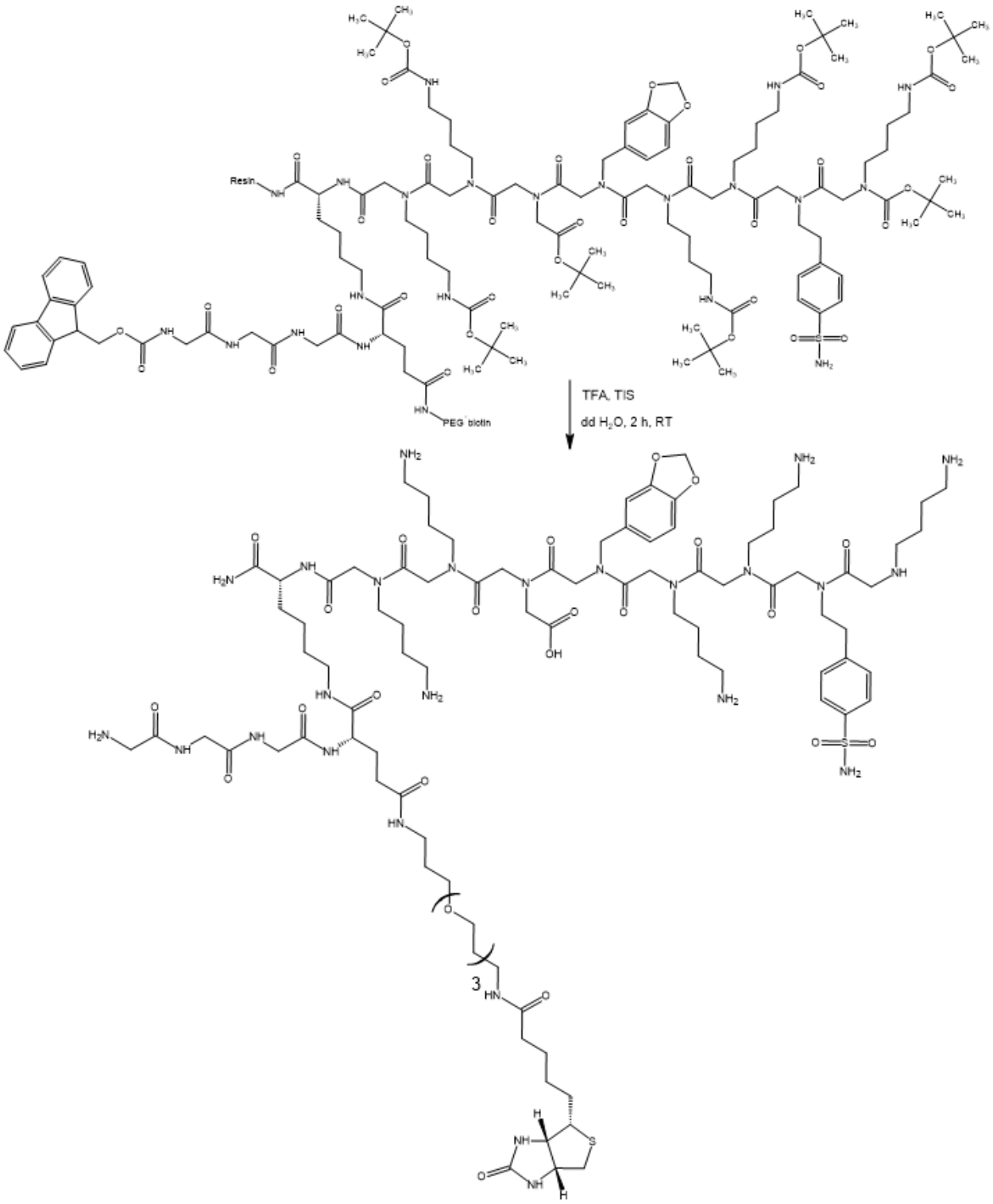

Figure 3.5. Part five of the BCSC targeting compound synthesis, showing the final product with the full structure of PEG-biotin.

Analytical HPLC of the synthesis product showed that multiple compounds were present (Figure 3.6 A), so preparatory HPLC was used to separate the synthesis product solution into fractions (Figure 3.6 B). The fractions were then analyzed using LC-MS, showing that three of the fractions contained either the desired compound, or a derivative of it. The first contained a mass equal to the compound with an extra oxygen, possibly due to oxidation of the sulfur on the biotin group (Figures 3.7 A and B). The second contained a mass equal to the desired compound (Figures 3.8 A and B). And the third contained a mass equal to the compound with a currently unknown addition (Figures 3.9 A and B).

LC-MS of the fraction containing the desired compound showed that other products were still present, so a second preparatory HPLC was used to purify it further (Figure 3.10). Analytical HPLC of the final fraction showed that the desired compound had been mostly purified (Figure 3.11), which LC-MS analysis confirmed (Figures 3.12 A and B).

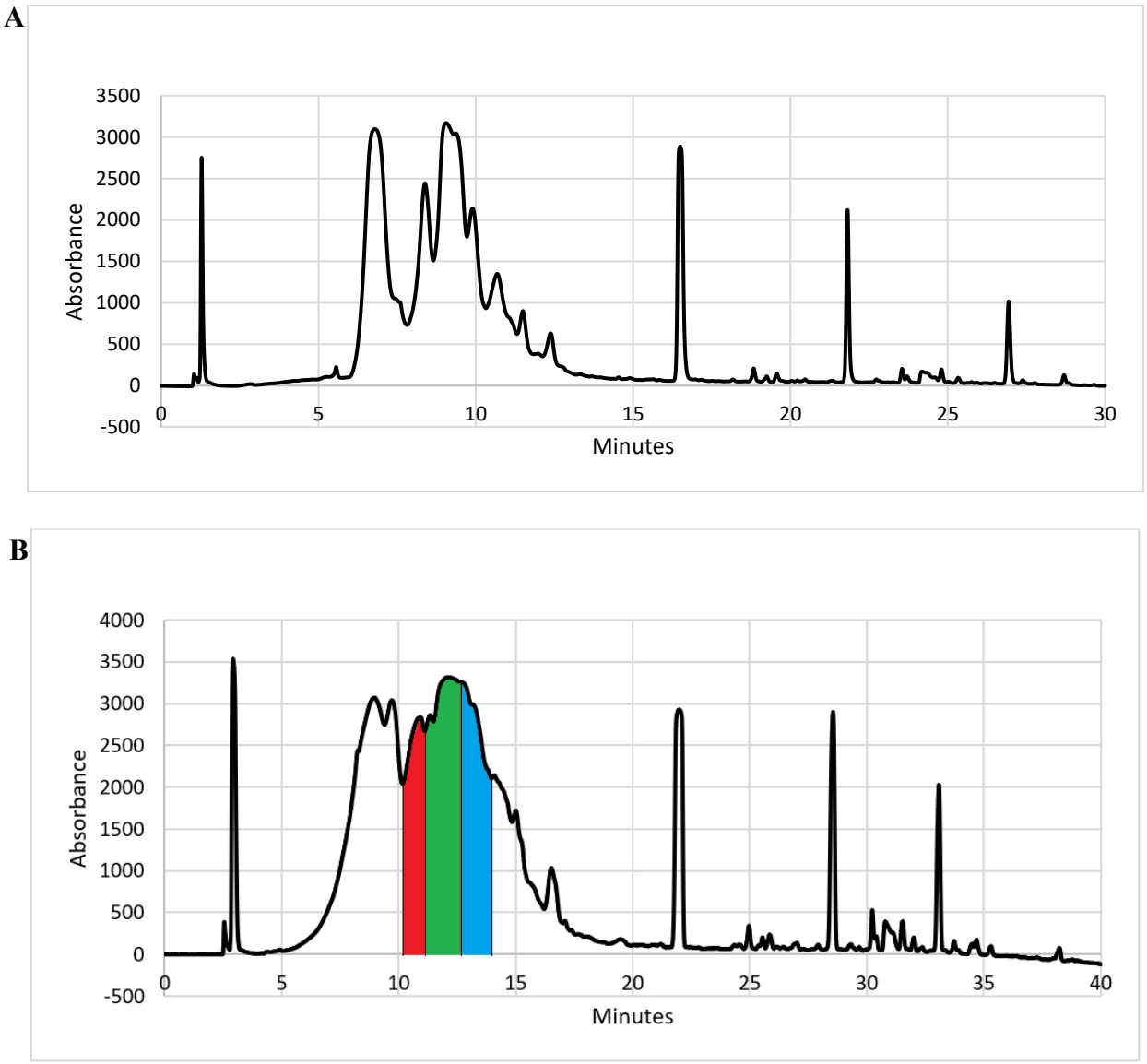

Figure 3.6. A: Analytical HPLC graph of the BCSC targeting compound synthesis product, showing that many different compounds were present. B: Preparatory HPLC graph showing the fractions containing the desired product or its derivatives.

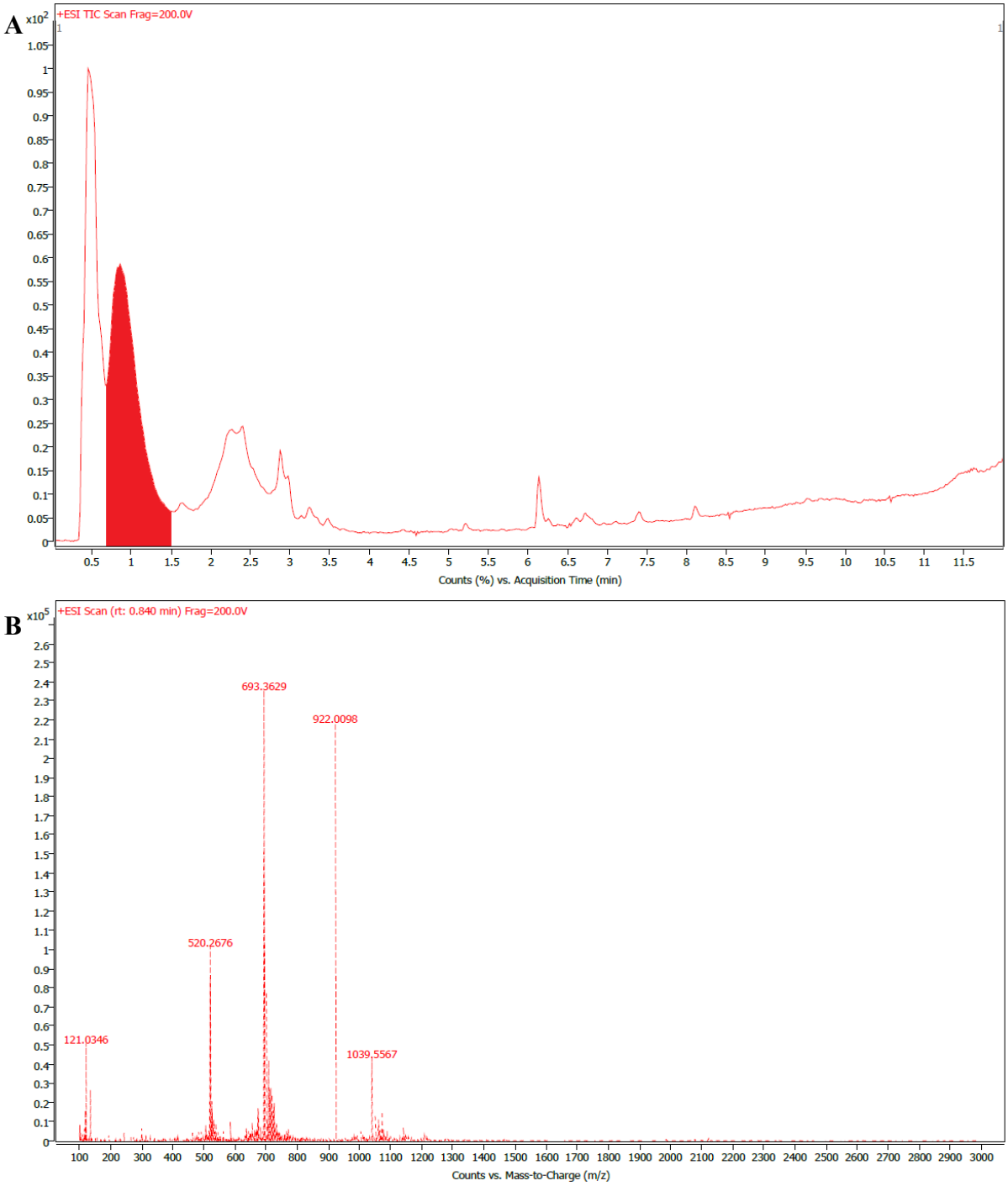

Figure 3.7. LC-MS chromatogram of an HPLC fraction containing a mass equal to the BCSC targeting compound with an extra oxygen (A). The shaded peak showed m/z ratios greater than the desired compound (B). The theoretical $[M+2]^+$, $[M+3]^+$, and $[M+4]^+$ m/z are 1031.736, 688.157, and 516.3678 respectively, while the observed values were 1039.5567, 693.3629, and 520.2676 respectively.

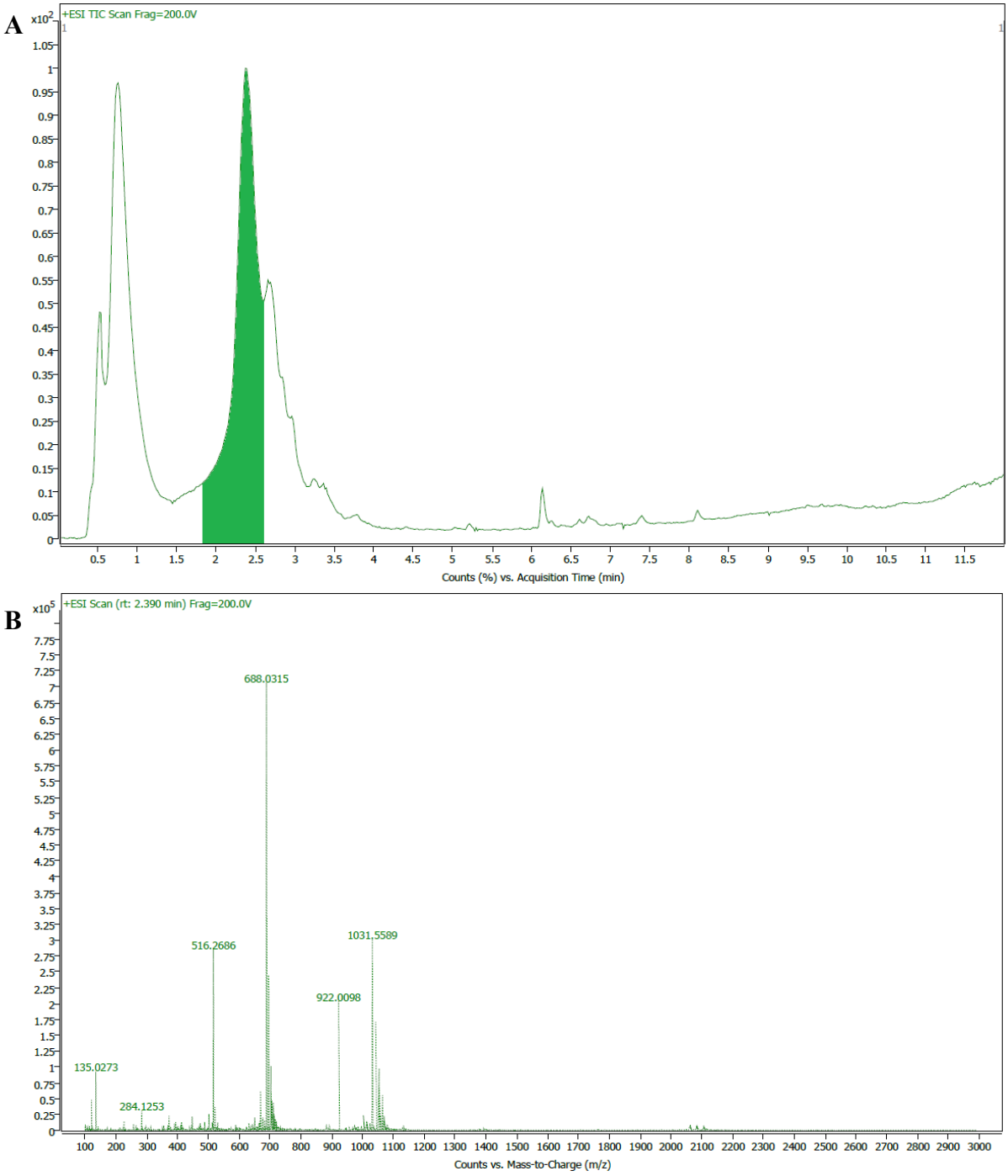

Figure 3.8. LC-MS chromatogram of an HPLC fraction containing a mass equal to the BCSC targeting compound (A). The shaded peak showed m/z ratios matching the desired compound (B). The theoretical $[M+2]^+$, $[M+3]^+$, and $[M+4]^+$ m/z are 1031.736, 688.157, and 516.3678 respectively, while the observed values were 1031.5589, 688.0315, and 516.2686 respectively.

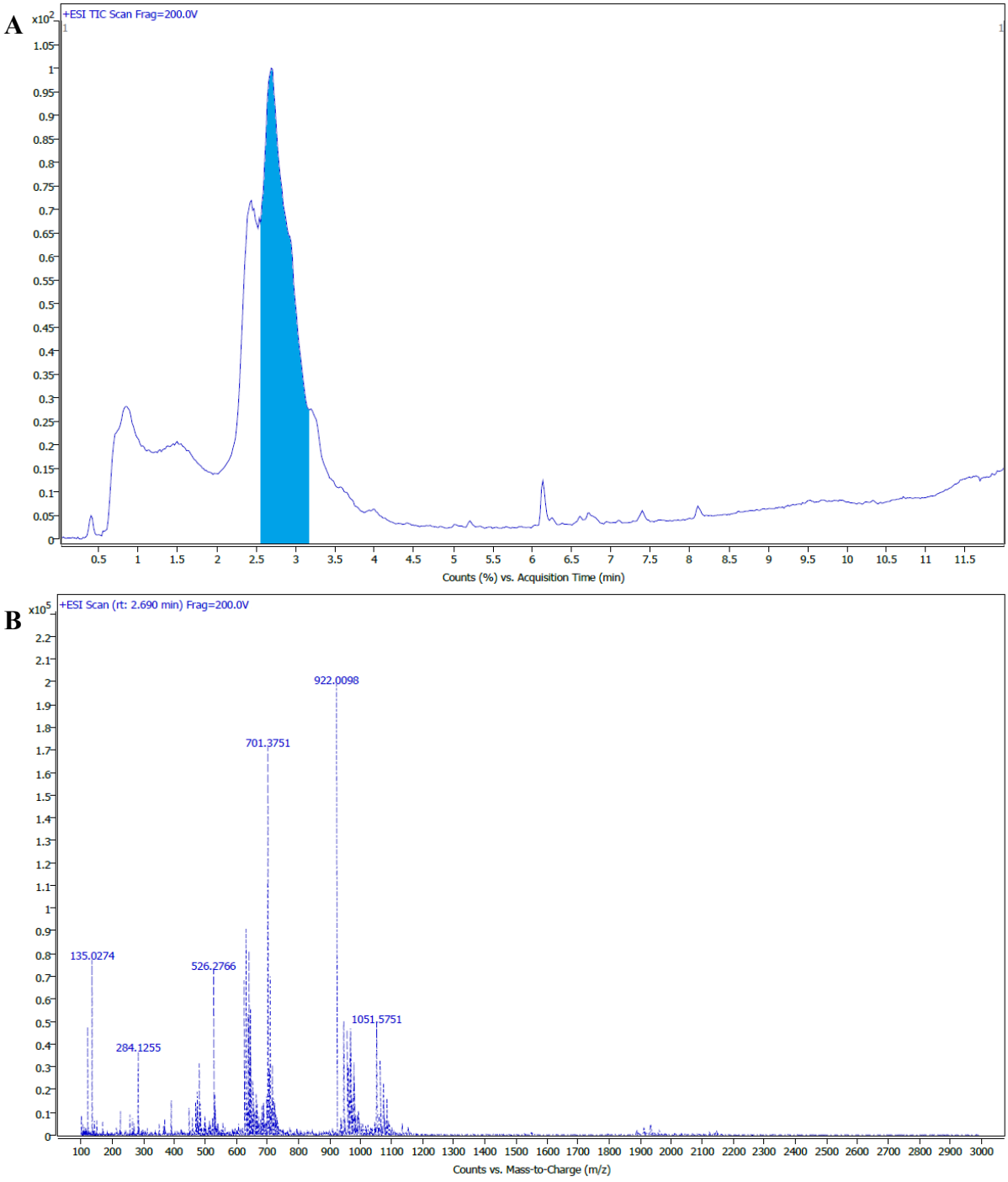

Figure 3.9. LC-MS chromatogram of an HPLC fraction containing a mass equal to the BCSC targeting compound with a currently unknown modification (A). The shaded peak showed m/z ratios greater than both the desired compound and the possibly oxidized derivative (B). The theoretical $[M+2]^+$, $[M+3]^+$, and $[M+4]^+$ m/z are 1031.736, 688.157, and 516.3678 respectively, while the observed values were 1051.5751, 701.3751, and 526.2766 respectively.

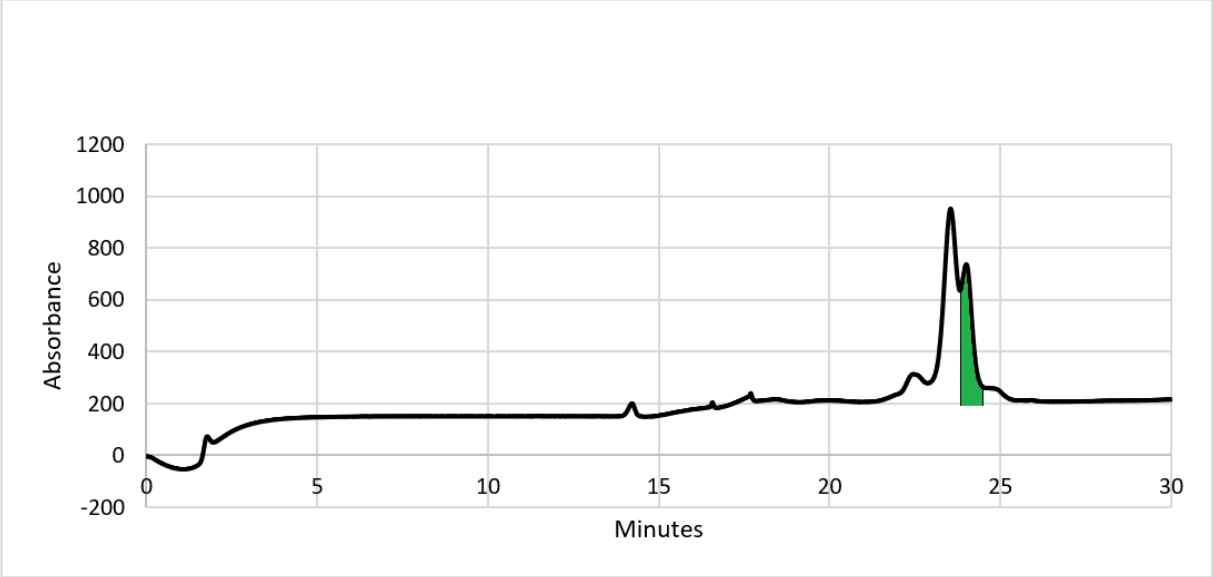

Figure 3.10. Preparatory HPLC graph of the fraction with the desired compound. The shaded peak contained the desired compound.

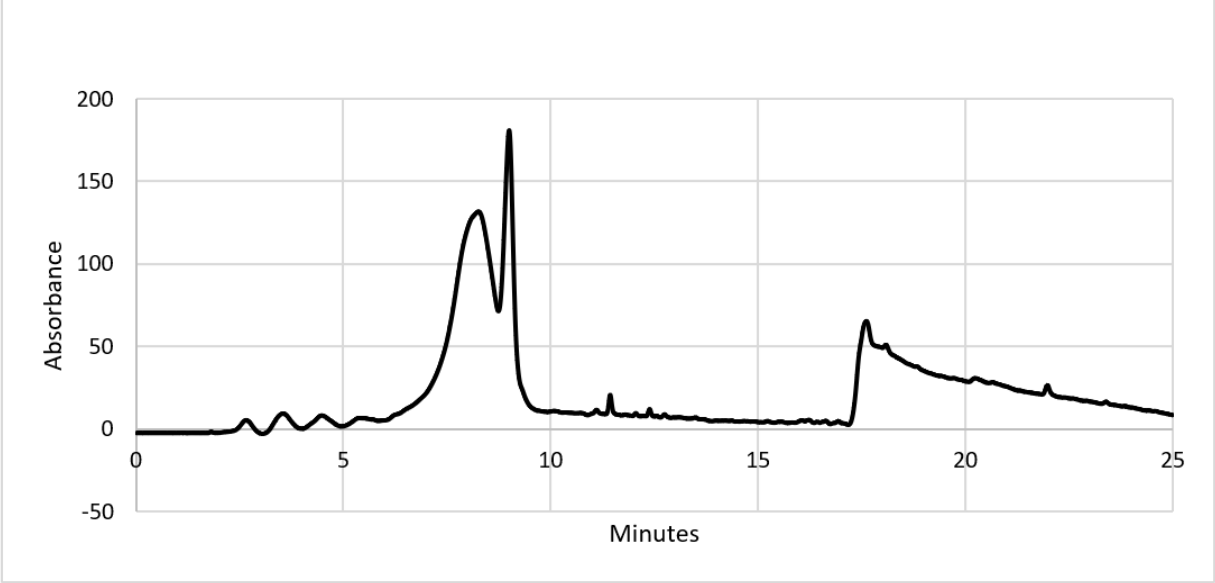

Figure 3.11. Analytical HPLC graph of the purified compound. The peak with the greatest area contained the desired compound.

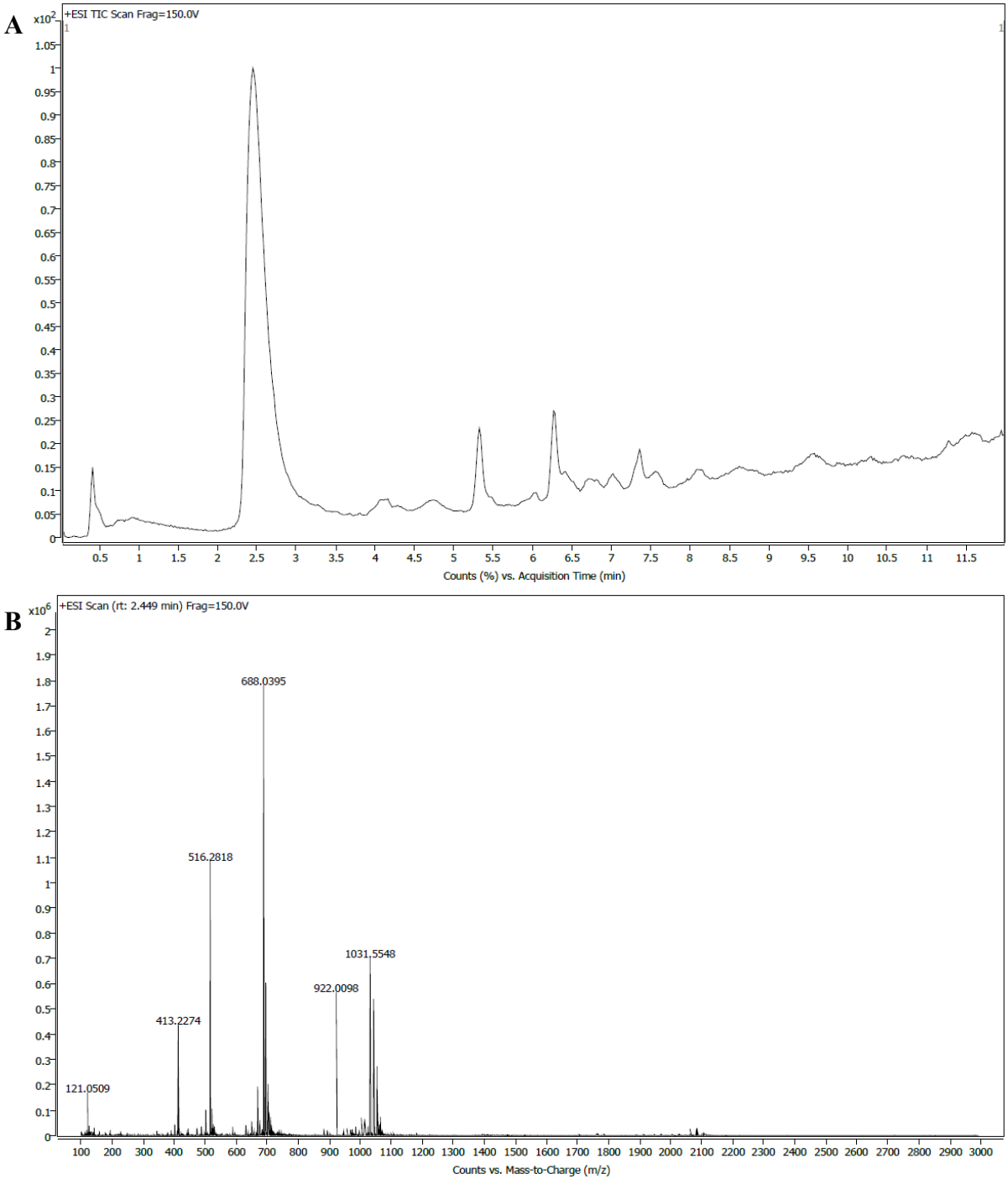

Figure 3.12. LC-MS chromatogram of the final purified compound showing little other product remaining (A). The major peak showed m/z ratios matching the desired compound (B). The theoretical $[M+2]^+$, $[M+3]^+$, and $[M+4]^+$ m/z are 1031.736, 688.157, and 516.3678 respectively, while the observed values were 1031.5548, 688.0395, and 516.2818 respectively.

3.2 Conjugation of the HK-97 VLP to the Synthetic Targeting Compound

For initial testing of the reaction conditions for conjugation of HK-97 VLP to the targeting compound, we used a Triple Negative Breast Cancer (TNBC) targeting compound while the BCSC targeting compound was being purified. It is similar to the BCSC targeting compound, consisting of a peptoid chain bound to both a polyglycine sequence and a PEG-biotin marker. The procedure used for conjugation was modified from a study looking at the conjugation of proteins to the bacteriophage P22 VLP.[19]

First, molar ratios of (1, 0.5, 0.1, 0.05, 0.025):1:1 for the TNBC targeting compound, sortase, and VLP subunit respectively were mixed at 42°C for three hours in 50 mM Tris (pH 8.0) with 6mM $CaCl_2$, then quenched with EDTA at a concentration of 6mM to remove the calcium. A spin desalting column with a 7k molecular weight cut-off was then used to filter out the EDTA and any remaining TNBC targeting compound.

Dot blot analysis was performed using a PVDF blotting membrane with 0.45 μg, 0.045 μg, and 0.015 μg loading. It was rocked in 5% BSA in TBST solution for 1 hour at RT to reduce non-specific binding, then rocked in a 1:40,000 NeutrAvidin-HRP conjugate in 1% BSA in TBST solution for 1 hour at RT which caused the NeutrAvidin-HRP conjugate to bind to the biotin group on the BCSC targeting compound. It was then washed several times with TBST, TBS, and finally DI water. Then a solution containing a peroxide reagent and a luminol reagent was applied to the membrane for 5 minutes at RT while covered. The peroxide reagent allows the HRP enzyme to catalyze the oxidation of the luminol, causing chemiluminescence. Viewing the dot blot with an imager showed that conjugation of the TNBC targeting compound to VLP had occurred and that the signal is dependent on the amount of targeting compound present (Figure 3.13).

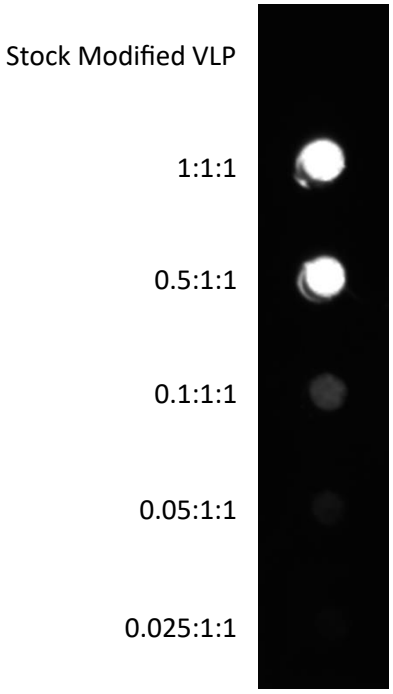

Figure 3.13. Dot blot analysis of stock modified VLP and TNBC Targeting Compound-VLP conjugates with different Compound:Sortase:VLP molar ratios. 0.45µg, 0.045µg, and 0.015µg loading was used.

3.3 Conjugation of the HK-97 VLP to Aldoxorubicin

For initial conjugation testing of HK-97 VLP to Aldoxorubucin, 4:1 Aldoxorubicin to VLP subunit, and 4:1 Doxorubicin to VLP subunit molar ratios were used. They were mixed by rocking at room temperature for two hours while protected from light to prevent the degradation of doxorubicin. A spin desalting column with a 7k molecular weight cut-off was used to filter out any remaining reactants.

SDS-PAGE of the conjugate solutions showed that the Aldoxorubicin conjugation was successful, and that Doxorubicin did not conjugate (Figure 3.14). DLS of the solutions showed that conjugation with Aldoxorubicin did not significantly alter the size of the VLP, though a small amount of aggregates or dust seemed to be present (Figures 3.15 A, B, and C).

To find the percentage of labeling that had occurred, and whether Aldoxorubicin is binding exclusively to the cysteines in the VLP, two conjugate solutions were made using the same method as before. One solution contained Aldoxorubicin with the cysteine modified VLP, while the other solution had Aldoxorubicin with Wild Type HK-97 VLP (WT VLP). The VLP in both conjugation reaction solutions were denatured by adding 6M Guanidine Hydrochloride (pH 7.4), shaking briefly, and allowing them to sit for one hour at room temperature. UV absorbance of the solutions showed that cysteine modified VLP had 107 percent labeling, while the WT VLP had 29 percent labeling (Figure 3.16), though the low concentrations used may have affected these percentages. While non-specific binding did occur, possibly on endogenous cysteines, the cysteine modified VLP showed a much higher percentage of binding compared to the WT VLP.

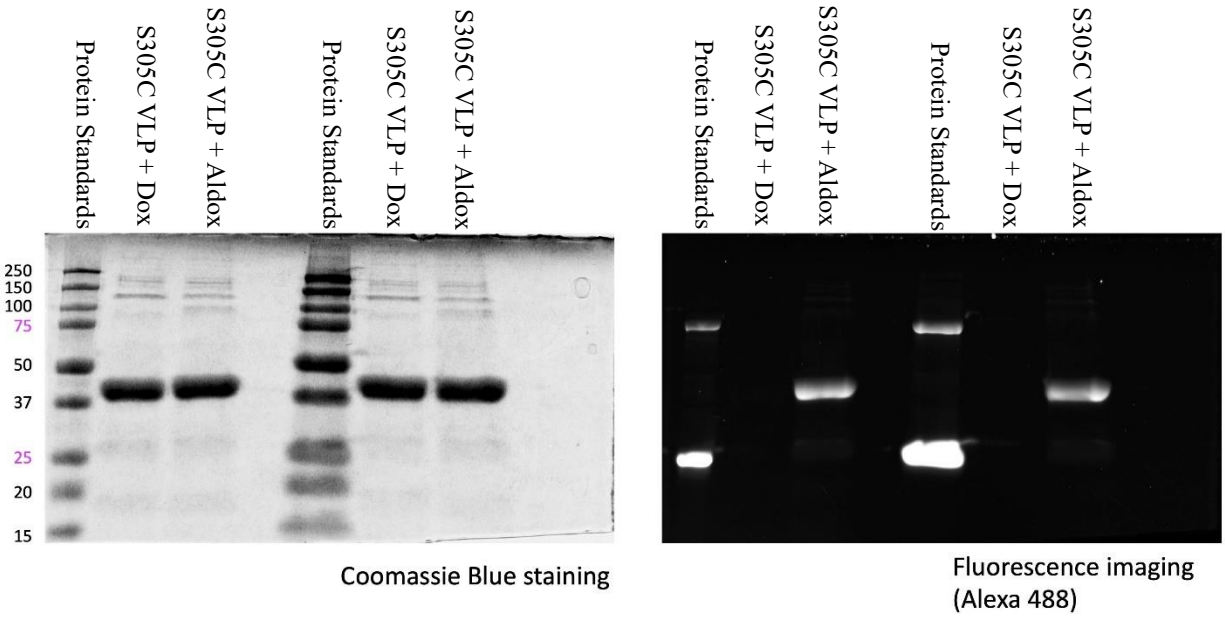

Figure 3.14. SDS-PAGE of the VLP from the Aldoxorubicin and VLP reaction solution (0.021 mg loading), and the Doxorubicin and VLP reaction solution (0.018 mg loading).

A

Sample	Z-Average (d. nm)	PDI	Peak 1 (d. nm, %V)
Aldox-VLP	62.28	0.195	49.00, 98.4
Dox-VLP	55.18	0.052	49.72, 100.0

B

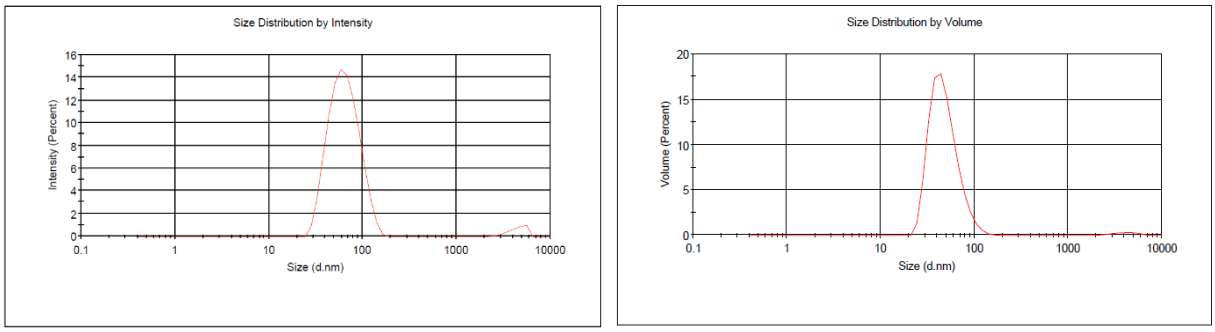

C

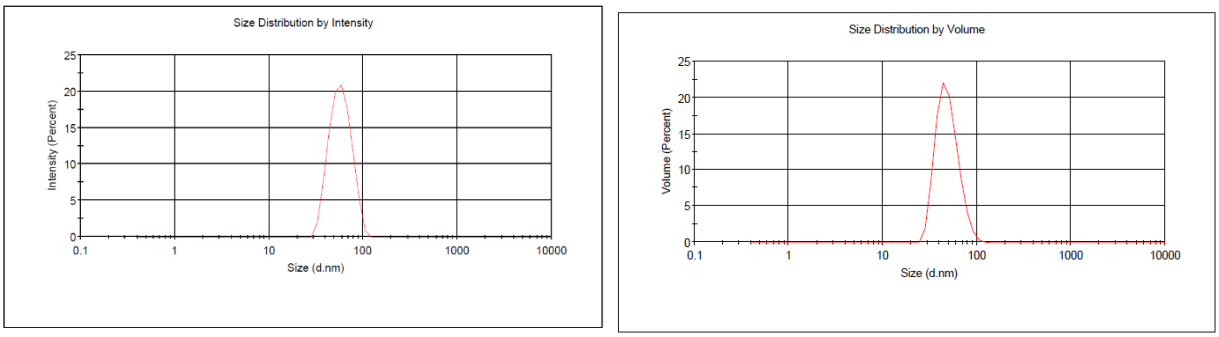

Figure 3.15. DLS data of Aldoxorubicin and Doxorubicin VLP reaction solutions showing the average diameter (Z-Average), the amount of non-uniformity (PDI), the average diameter of the first peak, and the approximate volume percent of the first peak for the overall sample (A). DLS graphs showing the percent size distribution by intensity and volume of the Aldoxorubicin and VLP reaction solution (B), and of the Doxorubicin and VLP reaction solution (C).

Sample	A_{280}	A_{495}	Dox (μM)	VLP (μM)
Aldox-VLP	0.0885	0.0197	2.13	1.984
Aldox-WT VLP	0.0865	0.0059	0.638	2.193

Figure 3.16. The UV absorbance and corresponding concentrations of Doxorubicin and VLP after Aldoxorubicin conjugation reaction with cysteine modified and wild type VLP, and filtering of excess Aldoxorubicin. The theoretical 100% Doxorubicin labeling concentration should be equal to the VLP concentration. Pathlength: 1cm. Doxorubicin Extinction Coefficient: 9250. VLP Extinction Coefficient: 37530.

3.4 Release of Doxorubicin in Acidic Conditions

To test the ability of the acid labile linker EMCH to release Doxorubicin, Aldoxorubicin-VLP conjugates were placed in acidic conditions to simulate the internal conditions of lysosomes.

To do this, Aldoxorubicin conjugated VLP was added to PBS (pH 5.0), and shaken gently at 37° C in the dark. A sample was taken after 1, 2, 3, 4, 5, 7, 9, 12, 20.5, 30, and 45.5 hours, then filtered with a 10 kDa molecular weight cut-off centrifugal filter to remove the VLP. The Doxorubicin concentration for each sample was determined by using fluorescence and a concentration curve, with excitation at 470 nm, and emission at 560 nm.

Fluorescence data showed that Doxorubicin was released at a steady pace for about the first 10 hours before slowing down and peaking at around 90% of the theoretical labeling amount (Figure 3.17).

A

Hours	1	2	3	4	5	7	9	12	20.5	30	45.5
Release (μM)	0.096	0.124	0.153	0.157	0.150	0.221	0.277	0.268	0.312	0.353	0.365
% Release	24.56	31.58	38.93	39.94	38.17	56.15	70.56	68.16	79.42	89.91	92.86

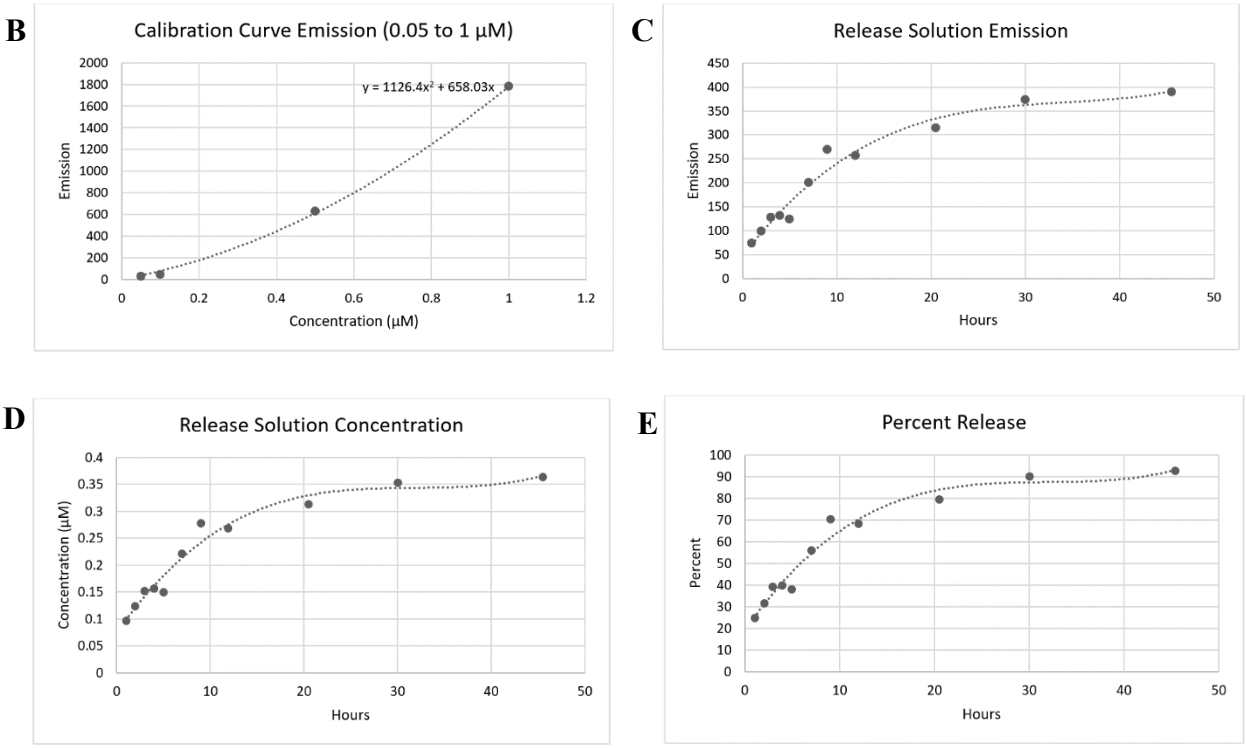

Figure 3.17. Fluorescence of the VLP-Aldoxorubicin conjugate solution over time in acidic conditions. The fluorescence excitation and emission wavelengths were 470 nm and 560 nm respectively. The theoretical concentration for 100% Doxorubicin release was 0.393 μM. A chart showing the Doxorubicin release concentration over time and its percentage of the theoretical amount of conjugated Doxorubicin (A). The emission values for the Doxorubicin calibration curve with concentrations of 0.05μM, 0.1μM, 0.5μM, 1μM (B). The emission value of the conjugate solution over time (C). The corresponding Doxorubicin concentration of the conjugate solution over time (D). The percent release of conjugated Doxorubicin over time relative to the theoretical total amount (E).

3.5 Conjugation of the HK-97 VLP to both Aldoxorubicin and Targeting Compound

For the full conjugation of HK-97 VLP, the BCSC targeting compound was conjugated to the VLP first. The reaction conditions remained the same as before, except a 1:1:1 BCSC targeting compound, sortase, and VLP subunit molar ratio was used instead of 0.5:1:1 ratio. Ultra-centrifugation was used instead of a spin desalting column to remove sortase, EDTA, and any extra BCSC targeting compound. PBS (pH 7.4) was used to dilute the sample after ultra-centrifugation to set up the buffer conditions for the Aldoxorubicin and VLP conjugation reaction.

Dot blot analysis of the conjugate followed the same procedure as before and showed that the conjugation was successful (Figure 3.18 A).

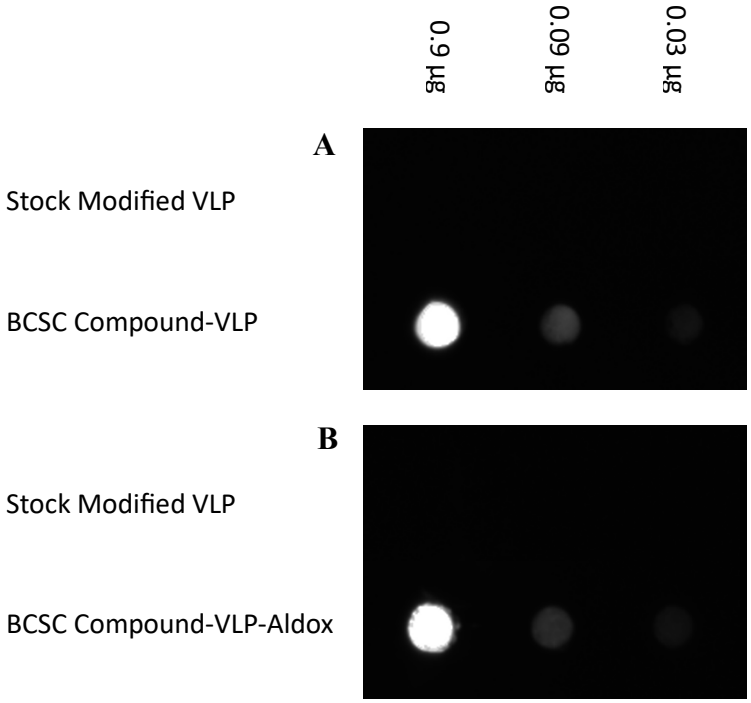

Figure 3.18. Dot blot analysis of the BCSC targeting compound conjugated to VLP, and stock modified VLP with 0.9µg, 0.09µg, and 0.03µg loading (A). Dot blot of VLP conjugated to both Aldoxorubicin and the targeting compound, and stock modified VLP with 0.9µg, 0.09µg, and 0.03µg loading (B).

Next, Aldoxorubicin was conjugated to the VLP conjugate. Reaction conditions were the same as mentioned previously, using a 4:1 Aldoxorubicin to VLP subunit ratio. A spin desalting column with a 7k molecular weight cut-off was used to remove any excess Aldoxorubicin.

Dot blot analysis of the final conjugate followed the same procedure as before, and showed that the BCSC targeting compound had remained conjugated to the VLP (Figure 3.18 B). DLS of the final conjugate solution showed that aggregation had occurred, possibly due to using ultracentrifugation (Figure 3.19).

A

Sample	Z-Average	PDI	Peak 1 (nm)	Peak 1 (%V)
Stock Modified VLP	59.01	0.097	59.01	100
BCSC Compound-VLP-Aldox	252.7	0.466	70.75	23.9

B

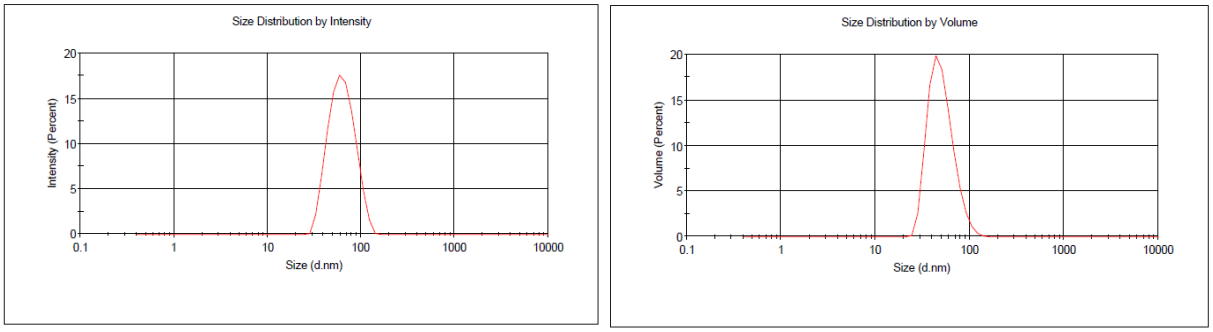

C

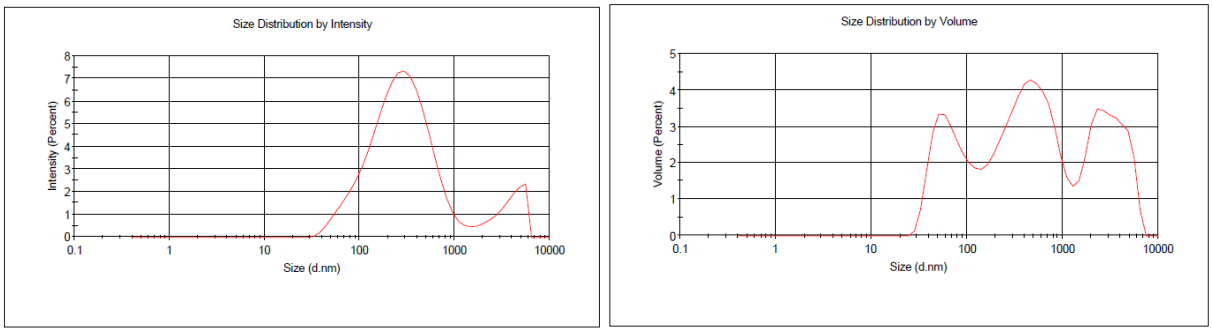

Figure 3.19. DLS data of the full BCSC targeting conjugate and stock modified VLP showing the average diameter (Z-Average), the amount of non-uniformity (PDI), the average diameter of the first peak, and the approximate volume percent of the first peak for the overall sample (A). DLS graphs showing the percent size distribution by intensity and volume of a stock modified VLP solution (0.085 mg/mL) (B), and of the BCSC targeting conjugate solution (0.079 mg/mL) (C).

3.6 Testing of the Conjugates on Cancer Cell Lines

In the future, testing of the BCSC targeting conjugate on MCF-7 and MDA-MB-231 breast cancer cell lines will be conducted. Both cell lines are known to contain a BCSC population.[13] The presence of doxorubicin in the cells will be viewed with a fluorescence microscope, and the viability of the cells will be monitored.

3.7 Conclusion

These experiments have shown that the conjugation of an acid labile chemotherapeutic drug and a cell specific binding compound to a modified HK-97 VLP is possible, and sets up the basic synthesis pathway to accomplish it. Cell testing showing the specificity and lethality of the conjugates, and the ability to conjugate other cell specific compounds and payloads is needed, along with optimization of the reaction and purification conditions. Hopefully in the future this research will lead to a new method of breast cancer treatment, and will be able to be modified to treat other types of cancer as well.

Chapter 4

Materials and Methods

4.1 Synthesis of the BCSC Synthetic Binding Compound

4.1.1 Preparation of the Resin and Addition of Fmoc-Lys(Alloc)-OH

50 mg of Rink Amide MBHA Resin was added to a 6 mL fritted syringe, rinsed with DMF, then placed in an orbital shaker to swell for 1.5 hours at RT in 0.6 mL of DMF. The DMF was drained, and 0.6 mL of 20% piperidine was added. This was placed in an orbital shaker for 20 minutes at RT. The solution was drained, then the resin was washed with DMF three times. 0.6 mL of 20% piperidine was added, and the resin was put on the orbital shaker for another 20 minutes at RT. The solution was drained, then the resin was washed with; DMF four times, MeOH two times, CH_2Cl_2 two times, then DMF another four times, and finally left in DMF. The coupling reagent solution was made using; 40 mg of Fmoc-Lys(Alloc)-OH, 13.6 mg of HOBt, 33.55 mg of HBTU, 0.5 mL of DMF, mixed until clear, then added 31 μL of DIPEA, and mixed until clear. The DMF was drained from the resin, the coupling reagent solution was added (about 550 μL), then the resin was shaken on an orbital shaker for 3 hours at RT. The resin was washed with; DMF four times, MeOH two times, CH_2Cl_2 two times, then DMF another four times. It was then washed with CH_2Cl_2 ten times, dried, sealed, then stored at 4°C.

4.1.2 Addition of Boc-diaminobutane (1st Peptoid Residue)

0.6 mL of DMF was added to the resin and placed on an orbital shaker for 1.5 hours at RT. The DMF was drained, and 0.6 mL of 20% piperidine was added. This was placed in an orbital shaker for 20 minutes at RT. The solution was drained, then the resin was washed

with DMF three times. 0.6 mL of 20% piperidine was added, and the resin was put on the orbital shaker for another 20 minutes at RT. The solution was drained, then the resin was washed with; DMF four times, MeOH two times, CH_2Cl_2 two times, then DMF another four times, and finally left in DMF. A CAA solution was made using 20 mg of CAA and 528 µL of DMF. A DIC solution was made using 41 µL of DIC and 90 µL of DMF. The DMF was drained, then 503 µL of CAA solution and 120 µL of DIC solution were added to the resin. It was shaken in an orbital shaker for 6 minutes at 35°C then was drained. The resin was washed with; DMF four times, MeOH two times, CH_2Cl_2 two times, then NMP four times, and finally left in NMP. A 1 Molar Boc-diaminobutane solution was prepared using 96 mg of Boc-diaminobutane and 408 µL of NMP. The NMP was drained from the syringe, and 504 µL of the Boc-diaminobutane solution was added. It was shaken on an orbital shaker for 3 hours at 35°C. The resin was washed with; DMF four times, MeOH two times, CH_2Cl_2 two times, then DMF another four times. It was then washed with CH_2Cl_2 ten times, dried, sealed, then stored at 4°C.

4.1.3 Addition of Boc-diaminobutane (2nd Peptoid Residue)

0.6 mL of DMF was added to the resin and placed on an orbital shaker for 1.5 hours at RT. A CAA solution was made using 20 mg of CAA and 528 µL of DMF. A DIC solution was made using 41 µL of DIC and 90 µL of DMF. The DMF was drained, then 503 µL of CAA solution and 120 µL of DIC solution were added to the resin. It was shaken in an orbital shaker for 6 minutes at 35°C then was drained. The resin was washed with; DMF four times, MeOH two times, CH_2Cl_2 two times, then NMP four times, and finally left in NMP. A 1 Molar Boc-diaminobutane solution was prepared using 96 mg of Boc-diaminobutane and 408 µL of NMP. The NMP was drained from the syringe, and 504 µL of the Boc-diaminobutane solution

was added. It was shaken on an orbital shaker for 3 hours at 35°C. The resin was washed with; DMF four times, MeOH two times, CH_2Cl_2 two times, then DMF another four times. It was then washed with CH_2Cl_2 ten times, dried, sealed, then stored at 4°C.

4.1.4 Addition of H-Gly-OtBu (3rd Peptoid Residue)

0.6 mL of DMF was added to the resin and placed on an orbital shaker for 1.5 hours at RT. A CAA solution was made using 20 mg of CAA and 528 µL of DMF. A DIC solution was made using 41 µL of DIC and 90 µL of DMF. The DMF was drained, then 503 µL of CAA solution and 120 µL of DIC solution were added to the resin. It was shaken in an orbital shaker for 6 minutes at 35°C then was drained. The resin was washed with; DMF four times, MeOH two times, CH_2Cl_2 two times, then NMP four times, and finally left in NMP. A 2 Molar H-Gly-OtBu solution was prepared using 153 µL of H-Gly-OtBu and 351 µL of NMP. The NMP was drained from the syringe, and 504 µL of the H-Gly-OtBu solution was added. It was shaken on an orbital shaker for 1.5 hours at 35°C. The resin was washed with; DMF four times, MeOH two times, CH_2Cl_2 two times, then DMF another four times. It was then washed with CH_2Cl_2 ten times, dried, sealed, then stored at 4°C.

4.1.5 Addition of piperonylamine (4th Peptoid Residue)

0.6 mL of DMF was added to the resin and placed on an orbital shaker for 1.5 hours at RT. A CAA solution was made using 20 mg of CAA and 528 µL of DMF. A DIC solution was made using 41 µL of DIC and 90 µL of DMF. The DMF was drained, then 503 µL of CAA solution and 120 µL of DIC solution were added to the resin. It was shaken in an orbital shaker for 6 minutes at 35°C then was drained. The resin was washed with; DMF four times,

MeOH two times, CH_2Cl_2 two times, then NMP four times, and finally left in NMP. A 2 Molar piperonylamine solution was prepared using 126 µL of piperonylamine and 378 µL of NMP. The NMP was drained from the syringe, and 504 µL of the piperonylamine solution was added. It was shaken on an orbital shaker for 1.5 hours at 35°C. The resin was washed with; DMF four times, MeOH two times, CH_2Cl_2 two times, then DMF another four times. It was then washed with CH_2Cl_2 ten times, dried, sealed, then stored at 4°C.

4.1.6 Addition of Boc-diaminobutane (5th Peptoid Residue)

This step followed the procedure previously listed in 4.1.3.

4.1.7 Addition of Boc-diaminobutane (6th Peptoid Residue)

This step followed the procedure previously listed in 4.1.3.

4.1.8 Addition of 4-(2-Aminoethyl)benzenesulfonamide (7th Peptoid Residue)

0.6 mL of DMF was added to the resin and placed on an orbital shaker for 1.5 hours at RT. A CAA solution was made using 20 mg of CAA and 528 µL of DMF. A DIC solution was made using 41 µL of DIC and 90 µL of DMF. The DMF was drained, then 503 µL of CAA solution and 120 µL of DIC solution were added to the resin. It was shaken in an orbital shaker for 6 minutes at 35°C then was drained. The resin was washed with; DMF four times, MeOH two times, CH_2Cl_2 two times, then NMP four times, and finally left in NMP. A 2 Molar 4-(2-Aminoethyl)benzenesulfonamide solution was prepared using 202 mg of 4-(2-Aminoethyl)benzenesulfonamide and 302 µL of NMP. The NMP was drained from the syringe, and 500 µL of the 4-(2-Aminoethyl)benzenesulfonamide solution was added. It was shaken on

an orbital shaker for 3 hours at 35°C. The resin was washed with; DMF four times, MeOH two times, CH_2Cl_2 two times, then DMF another four times. It was then washed with CH_2Cl_2 ten times, dried, sealed, then stored at 4°C.

4.1.9 Addition of Boc-diaminobutane (8th Peptoid Residue)

This step followed the procedure previously listed in 4.1.3.

4.1.10 Boc Protection of the Terminal Secondary Amine

0.6 mL of DMF was added to the resin and placed on an orbital shaker for 1 hour at RT. The reaction solution was made using 65.5 mg of $(Boc)_2O$, 0.5 mL of DMF, and 97 µL of Pyridine. The DMF was drained from the syringe, then the reaction solution was added (about 600 µL). It was shaken on an orbital shaker for 3 hours at RT. The resin was washed with; DMF four times, MeOH two times, CH_2Cl_2 two times, then DMF another four times. It was then washed with CH_2Cl_2 ten times, dried, sealed, then stored at 4°C.

4.1.11 Alloc Deprotection and Addition of Fmoc-Gln(biotinyl)-PEG-OH

0.8 mL of dry CH_2Cl_2 was added to the resin and placed on an orbital shaker for 30 minutes at RT. The deprotection solution was prepared using 7 mg of tetrakis(triphenylphosphine)palladium, 0.7 mL of dry CH_2Cl_2, and 93 µL of phenylsilane. The dry CH_2Cl_2 was drained from the syringe, and the deprotection solution was added. The syringe was shaken on an orbital shaker for 25 minutes at RT. The syringe was drained, then washed with dry CH_2Cl_2 three times. The deprotection and washing steps were repeated two more times. The resin was then washed with regular CH_2Cl_2 six times, DMF six times, then 0.6 mL of DMF

was added and the syringe was put on the orbital shaker for 5 minutes at RT. The coupling reagent solution was made using 72 mg of Fmoc-Gln(biotinyl)-PEG-OH, 14 mg of HOBt, 34 mg of HBTU, and 0.5 mL of DMF, which was then mixed before adding 63μL of DIPEA and mixing again. The DMF was drained from the syringe, then the coupling reagent solution was added. The syringe was shaken on an orbital shaker for 3 hours at RT. The resin was then washed with; DMF four times, MeOH two times, CH_2Cl_2 two times, then DMF another four times. It was then washed with CH_2Cl_2 ten times, dried, sealed, then stored at 4°C.

4.1.12 Addition of the Polyglycine

0.6 mL of DMF was added to the resin and placed on an orbital shaker for 1 hour at RT. The DMF was drained, and 0.6 mL of 20% piperidine was added. This was placed in an orbital shaker for 30 minutes at RT. The solution was drained, then the resin was washed with DMF three times. 0.6 mL of 20% piperidine was added, and the resin was put on the orbital shaker for another 10 minutes at RT. The solution was drained, then the resin was washed with; DMF four times, MeOH two times, CH_2Cl_2 two times, then DMF another four times, and finally left in DMF. The coupling reagent solution was made using 45 mg of Fmoc-Gly-OH, 23 mg of HOBt, 57 mg of HBTU, and 0.5 mL of DMF, which was then mixed before adding 52 μL of DIPEA and mixing again. The DMF was drained from the syringe, then the coupling reagent solution was added. The syringe was shaken on an orbital shaker for 2 hours at RT. The resin was then washed with; DMF four times, MeOH two times, CH_2Cl_2 two times, then DMF another four times. It was then washed with CH_2Cl_2 ten times, dried, sealed, then stored at 4°C. This procedure was done two more times.

4.1.13 Cleaving the Compound from the Resin

The resin was washed with CH_2Cl_2, drained, and dried. The cleaving solution was made using 1.9 mL of TFA, 0.05 mL of dd H_2O, and 0.05 mL of TIS. The solution was added to the syringe, which was then put on an orbital shaker for 2 hours at RT. The syringe was then drained into a vial, and washed with CH_2Cl_2. Nitrogen gas was blown into the vial to evaporate the TFA and CH_2Cl_2. Once dry, the vial was sealed and stored at -80° C.

4.1.14 Analytical HPLC of the Compound

For analytical HPLC of the targeting compound synthesis product, an Agilent Technologies 1260 Infinity HPLC with an Agilent Eclipse Plus C18 (3.5 µm) (4.6 x 100 mm) column was used. 20µL of sample was loaded, and 210 nm absorption was used. The method used was; from 100% dd water and 0% acetonitrile to 40% dd water and 60% acetonitrile over 25 minutes, then to 0% water and 100% acetonitrile over 15 minutes, then to 100% dd water and 0% acetonitrile over 10 minutes, all with a flow rate of 1 mL/minute.

4.1.15 Preparatory HPLC of the Compound

For preparatory HPLC of the targeting compound synthesis product, an Agilent Technologies 1260 Infinity HPLC with an Gemini-NX 5u C18 110Å AXI (250 x 21.2 mm) column was used. 250µL to 500µL of sample was loaded, and 210 nm absorption was used. The method used was; from 100% dd water and 0% acetonitrile to 25% dd water and 75% acetonitrile over 50 minutes, then to 0% water and 100% acetonitrile over 10 minutes, then to 100% dd water and 0% acetonitrile over 10 minutes, all with a flow rate of 5 mL/minute.

4.1.16 LC-MS of the Compound

For LC-MS of the targeting compound synthesis product, an Agilent 6230 LC/TOF using a 1260 Infinity II LC with an Agilent Extend-C18 (1.8µm) (2.1 x 50 mm) column was used. For settings, a 2µL injection volume, 0.4 mL/minute flow rate, 200V fragmentation voltage, 100 to 3000 m/z range, and 121.050873 and 922.009798 reference masses were used. 250 nm adsorption was used for examining the HPLC fractions, while 210 nm and 250 nm adsorption was used for examining the purified compound. The method used was; from 95% water and 5% acetonitrile to 5% water and 95% acetonitrile over 12 minutes with a 6 minute post time.

4.2 Conjugation of the Compound to VLP's

4.2.1 TNBC Targeting Compound Conjugation Reaction

To five Eppendorf tubes was added add 43 µL of 50mM Tris buffer (pH 8.0) with 6 mM CaCl, 0.3 µL of TNBC targeting compound in DMSO (2 mM, 1 mM, 0.2 mM, 0.1 mM, 0.05 mM), 2.7 µL of Sortase (220 µM), and 4 µL of LPETG modified HK-97 (151 µM) (6.4 mg/mL) VLP. The tubes were mixed gently for three hours at 42° C. To quench the reaction, 1.5 µL of 200 mM EDTA (pH 8.0) was added to each tube. The solutions were purified using Thermo Scientific 75 µL Zeba Spin Desalting Columns with a 7k MWCO. The columns were prepared by centrifuging at 1500g and 4° C for 1 minutes to remove the storage solution. Then 50 µL of 50mM Tris Buffer (pH 8.0) was added and centrifuged at the same conditions three times. The samples were then centrifuged at the same conditions, collected, then stored at 4° C.

4.2.2 Dot Blot Characterization

Made 0.15, 0.015, and 0.005 μg/μL concentrations of TNBC targeting compound-VLP conjugate solution, and VLP control solution, 50mM Tris Buffer (pH 8.0). The nitrocellulose membrane was pre-wet with TBS for 10 minutes, then was placed in a Bio-Rad Bio-Dot apparatus. Each well was washed with 100 μL of TBS before the sample was added and allowed to sit for 30 minutes. A vacuum was applied, then the membrane was removed and washed with TBST three times. Then the membrane was rocked in 5% BSA in TBST for one hour at room temperature. Added 0.625 μL of NeutrAvidin in 25 mL of 1% BSA in TBST to make a 1:40,000 solution, which the membrane was then rocked in for one hour at room temperature. The membrane was then rocked six times in TBST, and two times in TBS for five minutes each. It was then rinsed with DI Water. 1.4 mL of Clarity Western ECL Substrate solution was applied to the membrane, and allowed to sit at room temperature for 5 minutes. Used a Bio-Rad imager to view the membrane.

4.3 Conjugation of Aldoxorubicin to VLP's

4.3.1 Conjugation Reaction

Added 4.3 μL (21.4 nmol) of 5 mM Aldoxorubicin in DMSO solution and 500 μL of 10.7μM cysteine modified HK-97 VLP (5.35 nmol of VLP subunit) in PBS (pH 7.4) to an Eppendorf tube. Made a second Eppendorf tube with 5 mM Doxorubicin in DMSO as a control. Rocked tubes for two hours at room temperature while covered in foil. The solutions were purified using Thermo Scientific 2 mL Zeba Spin Desalting Columns with a 7k MWCO. The columns were prepared by centrifuging at 1000g and 4° C for 2 minutes to remove the storage

solution. Then 1 mL of PBS (pH 7.4) was added and centrifuged at the same conditions four times. The samples were then centrifuged at the same conditions, collected, then stored at 4° C.

4.3.2 UV Absorbance Characterization

Determined the Doxorubicin concentration of the sample using the UV absorbance at 495 nm and the following equation:

$$\text{Concentration} = \frac{\text{Abs}_{495\text{nm}}}{(\text{Optical path length})(9250\ \text{M}^{-1}\text{cm}^{-1})}$$

Determined the VLP subunit concentration using the UV absorbance at 280nm and 495 nm, and used the following equation to account for Doxorubicin absorbance at 280 nm:

$$\text{Concentration} = \frac{\text{Abs}_{280\text{nm}} - (0.713 \times \text{Abs}_{495\text{nm}})}{(\text{Optical path length})(37530\ \text{M}^{-1}\text{cm}^{-1})}$$

4.3.3 DLS Characterization

Added 185µL of Aldoxorubicin-VLP reaction solution (0.811 mg/mL) and 222µL of Doxorubicin-VLP reaction solution (0.676 mg/mL) to Eppendorf tubes. They were then diluted to 1 mL with PBS (pH 7.4) to get a VLP subunit concentration of 0.15 mg/mL. Checked the size of the VLP using a Zetasizer Nano-ZS DLS.

4.3.4 SDS-PAGE Characterization

Added 25µL of 4x SDS sample buffer to 75µL of Aldoxorubicin-VLP reaction solution (0.811 mg/mL) and 75µL of Doxorubicin-VLP reaction solution (0.676 mg/mL) to get final concentrations of 0.608 mg/mL and 0.507 mg/mL respectively. Boiled both solutions for 10

minutes. Prepared Bio-Rad Mini-Protean TGX Precast Gel in 10x Tris-Glycine running buffer. Added 35µL each of Bio-Rad Precision Plus Protein Dual Color Standards to wells 1 and 5, Doxorubicin-VLP to wells 2 and 6, and Aldoxorubicin-VLP to wells 3 and 7. Ran at 160V.

4.3.5 Denaturing Procedure

Added 200µL of Aldoxorubicin-VLP reaction solution, Aldoxorubicin-WT reaction solution, and PBS (pH 7.4) to separate Eppendorf tubes. Then added 800µL of 6M Guanidine Hydrochloride in PBS (pH 7.4) to all three tubes. Shook briefly, then let sit for one hour at room temperature. Stored at 4° C.

4.3.6 Fluorescence Measurements

Added 200µL of each sample to a well plate. Measured fluorescence using a plate reader. Excitation was at 470nm, and emission was at 560nm.

4.4 Testing the Release of Doxorubicin from VLP's

4.4.1 Release Procedure

Added 10 mL of PBS (pH 5.0) and 230 µL of Aldoxorubicin-VLP conjugate solution (0.811 mg/mL) to a 15 mL tube. Shook gently at 37° C in the dark. Took out 0.5 mL of the solution at 1h, 2h, 3h, 4h, 5h, 7h, 9h, 12h, 20h, 30h, and 45h. Each sample was put into an Eppendorf tube with a 10 kDa molecular weight cut-off Microcon centrifugal filter to remove the VLP, and centrifuged for 15 min at 14000 rpm. Stored at 4° C.

4.4.2 Doxorubicin Calibration Curve

Made a 2.5 mM Doxorubicin solution using 4.9 mg of dox, 1.69 mL of PBS (pH 5.0), and 1.69 mL of DMSO. Used the 2.5 mM Doxorubicin solution and PBS (pH 5.0) to make a calibration curve of: 100μM, 50μM, 10μM, 5μM, 1μM, 0.5μM, 0.1μM, and 0.05μM. Stored at 4° C.

4.4.3 Fluorescence Measurements

Added 200μL of each sample and the Doxorubicin calibration curve to a well plate. Measured fluorescence using a plate reader. Excitation was at 470nm, and emission was at 560nm.

4.5 Conjugation of VLP's to Both Doxorubicin and the Compound

4.5.1 Conjugation Procedure

To an Eppendorf tube was added 854 μL of 50mM Tris buffer (pH 8) with 6 mM CaCl, 12 μL of BCSC targeting compound (1 mM), 54 μL of Sortase (220 μM), and 80 μL LPETG and cysteine modified HK-97 VLP (151 μM) (6.4 mg/mL) VLP. It was mixed gently for three hours at 42° C. To quench the reaction, 30 μL of 200 mM EDTA (pH 8.0) was added. The solution was diluted to about 25 mL with PBS (pH 7.4) then purified using ultracentrifugation at 38,000 rpm for one hour. The supernatant was poured off, and the sample was resuspended in the remaining solution. Added 1.84 μL (9.2 nmol) of 5 mM Aldoxorubicin in DMSO solution and 270 μL of 10.7 μM BCSC targeting compound-VLP (2.3 nmol of VLP subunit) in PBS (pH 7.4) to an Eppendorf tube. Rocked for two hours at room temperature while covered in foil. The solution was purified using Thermo Scientific 2 mL Zeba Spin Desalting Columns with a 7k

MWCO. The column was prepared by centrifuging at 1000g and 4° C for 2 minutes to remove the storage solution. Then 1 mL of PBS (pH 7.4) was added and centrifuged at the same conditions four times. The sample was then centrifuged at the same conditions, and collected. 80μL of PBS was added to the column and centrifuged again to recover more sample. It was then stored at 4° C.

4.5.2 Dot Blot Characterization

Made solutions containing 0.9μg 0.09μg, and 0.03μg, of VLP subunits for BCSC targeting compound conjugate, and stock modified VLP in 50μL of PBS. A nitrocellulose membrane was pre-wet in PBS for ten minutes, then secured in a Bio-Rad Bio-Dot apparatus. Then, 100μL of TBS was added to each well and drained. The samples were added, and allowed to drain by gravity for thirty minutes before a vacuum was applied. The membrane was removed from the apparatus, and washed with TBST three times. Then it was rocked in 5% BSA in TBST for one hour at room temperature. Added 0.625 μL of NeutrAvidin in 25 mL of 1% BSA in TBST to make a 1:40,000 solution, which the membrane was then rocked in for one hour at room temperature. The membrane was then rocked six times in TBST, and two times in TBS for five minutes each. It was then rinsed with DI Water. 1.4 mL of Clarity Western ECL Substrate solution was applied to the membrane, and allowed to sit at room temperature for 5 minutes. Used a Bio-Rad imager to view the membrane.

4.5.3 DLS Characterization

The BCSC targeting compound conjugate was diluted with PBS to 1 mL giving a concentration of 0.079 mg/mL. A solution of 0.085 mg/mL LPETG and cysteine modified VLP in PBS was also made. Viewed on a Zetasizer Nano-ZS DLS.

References

1. Jordan C. T.; Guzman M. L.; Noble M. Cancer Stem Cells. *The New England Journal of Medicine* **2006**, *355*, 1253-1261. DOI: 10.1056/NEJMra061808
2. Shiozawa, Y.; Nie, B.; Pienta, K. J.; Morgan, T.M.; Taichman, R. S. Cancer stem cells and their role in metastasis. *Journal of Pharmacology & Therapeutics* **2013**, *138* (2), 285-293. DOI: 10.1016/j.pharmthera.2013.01.014
3. Li, Y.; Wang, Z.; Ajani, J. A.; Song, S. Drug resistance and Cancer stem cells. *Cell Communication and Signaling* **2021**, *19* (1), 19. DOI: 10.1186/s12964-020-00627-5
4. Al-Hajj, M.; Wicha, M. S.; Benito-Hernandez, A.; Morrison, S. J.; Clarke, M. F. Prospective identification of tumorigenic breast cancer cells. *Proceedings of the National Academy of Sciences of the United States of America* **2003**, *100* (7), 3983-3988. DOI: 10.1073/pnas.0530291100.
5. Li, S.; Li, Q. Cancer stem cells and tumor metastasis (Review) *International Journal of Oncology* **2014** *44* (6), 1806-1812. DOI:10.3892/ijo.2014.2362
6. Jin, L.; Hope, K. J.; Zhai, Q.; Smadja-Joffe, F.; Dick, J. E. Targeting of CD44 eradicates human acute myeloid leukemic stem cells. *Nature Medicine* **2006** *12*, 1167–1174. DOI:10.1038/nm1483
7. Marquardt, J. U.; Gomez-Quiroz, L.; Arreguin Camacho, L. O.; et al. Curcumin effectively inhibits oncogenic NF-kappaB signaling and restrains stemness features in liver cancer. *Journal of Hepatology* **2015** *63* (3), 661–669.
8. Pollyea, D. A.; Stevens, B. M.; Jones, C. L.; et al. Venetoclax with azacitidine disrupts energy metabolism and targets leukemia stem cells in patients with acute myeloid leukemia. *Nature Medicine* **2018** *24,* 1859–1866. DOI:10.1038/s41591-018-0233-1

9. Gupta, P. B.; Onder, T. T.; Jiang, G.; Tao, K.; Kuperwasser, C.; Weinberg, R. A.; Lander, E. S. Identification of selective inhibitors of cancer stem cells by high-throughput screening. *Cell* **2009** *138* (4), 645–659.

10. Mai, T. T.;, et al. Salinomycin kills cancer stem cells by sequestering iron in lysosomes. *Nature Chemistry* **2017** *9* (10), 1025–1033. DOI:10.1038/NCHEM.2778

11. Wu, C.; Hong, B.; Ho, C.; Yen, G. Targeting Cancer Stem Cells in Breast Cancer: Potential Anticancer Properties of 6-Shogaol and Pterostilbene. *Journal of Agricultural and Food Chemistry* **2015**, *63*, 2432−2441. DOI: 10.1021/acs.jafc.5b00002

12. Suntharalingam, K.; Lin, W.; Johnstone, T. C.; Bruno, P. M.; Zheng, Y.; Hemann, M. T.; Lippard, S. J. A Breast Cancer Stem Cell-Selective, Mammospheres-Potent Osmium(VI) Nitrido Complex. *Journal of the American Chemical Society* **2014**, *136*, 14413−14416. DOI: 10.1021/ja508808v

13. Chen, L.; Long, C.; Tran, K. A. M.; Lee, J. A Synthetic Binder of Breast Cancer Stem Cells. *Chemistry A European Journal* **2018**, *24*, 3694 – 3698. DOI: 10.1002/chem.201705663

14. Phillips, T. M.; McBride, W. H.; Pajonk, F. The response of $CD24^{-/low}$ /$CD44^{+}$ breast cancer–initiating cells to radiation. *Journal of the National Cancer Institute* **2006** *98* (24), 1777–1785. DOI:10.1093/jnci/djj495

15. Idowu, M. O.; Kmieciak, M.; Dumur, C.; Burton, R. S.; Grimes, M. M.; Powers, C.N.; Manjili, M. H. $CD44^{+}$/$CD24^{-/low}$ cancer stem/progenitor cells are more abundant in triple-negative invasive breast carcinoma phenotype and are associated with poor outcome. *Human Pathology* **2012** *43* (3), 364–373. DOI:10.1016/j.humpath.2011.05.005.

16. Al-Hajj, M; Wicha, M. S.; Benito-Hernandez, A.; Morrison, S. J.; Clarke, M. F.; Prospective identification of tumorigenic breast cancer cells. *Proceedings of the National Academy of Sciences of the United States of America USA* **2003** *100* (7), 3983–3988. DOI:10.1073/pnas.0530291100

17. Ginestier, C.; Hur, M. H.; Charafe-Jauffret, E.; Monville, F.; Dutcher, J.; Brown, M.; Jacquemier, J.; Viens, P.; Kleer, C. G.; Liu, S.; Schott, A.; Hayes, D.; Birnbaum, D.; M. Wicha, M. S.; Dontu, G. ALDH1 is a marker of normal and malignant human mammary stem cells and a predictor of poor clinical outcome. *Cell Stem Cell* **2007** *1* (5), 555–567. DOI:10.1016/j.stem.2007.08.014

18. Zhong, Y.; Shen, S.; Zhou, Y.; Mao, F.; Guan, J.; Lin, Y.; Xu, Y.; Sun, Q. ALDH1 is a better clinical indicator for relapse of invasive ductal breast cancer than the CD44+/CD24− phenotype. *Medical Oncology* **2014** *31* (3), 864. DOI:10.1007/s12032-014-0864-0

19. Patterson, D.; Schwarz, B.; Avera, J.; Western, B.; Hicks, M.; Krugler, P.; Terra, M.; Uchida, M.; McCoy, K.; Douglas, T. Sortase-Mediated Ligation as a Modular Approach for the Covalent Attachment of Proteins to the Exterior of the Bacteriophage P22 Virus-like Particle. *Bioconjugate Chemistry* **2017**, *28* (8), 2114-2124. DOI: 10.1021/acs.bioconjchem.7b00296

20. Rynda-Apple, A.; Patterson, D. P.; Douglas, T. Virus-like particles as antigenic nanomaterials for inducing protective immune responses in the lung. *Nanomedicine* **2014**, *9*, 1857−1868. DOI:10.2217/nnm.14.107

21. Al-Barwani, F.; Donaldson, B.; Pelham, S. J.; Young, S. L.; Ward, V. K. Antigen delivery by virus-like particles for immunotherapeutic vaccination. *Therapeutic Delivery* **2014** *5*, 1223−1240. DOI:10.4155/tde.14.74

22. Ma, Y.; Nolte, R. J. M.; Cornelissen, J. J. L. M. Virus-based nanocarriers for drug delivery. *Advanced Drug Delivery Reviews* **2012**, *64*, 811-825. DOI:10.1016/j.addr.2012.01.005

23. Maity, B.; Fujita, K.; and Ueno, T. Use of the confined spaces of apo-ferritin and virus capsids as nanoreactors for catalytic reactions. *Current Opinion in Chemical Biology* **2015** *25*, 88−97. DOI:10.1016/j.cbpa.2014.12.026

24. Woods, M. D.; Cali, M.; Ceesay, B.; Fancher, S.; Ibrasheva, G.; Kandeel, S.; Nassar, M.; Azghani, A.; Bill, B.; Patterson, D. P. Engineering the HK97 virus-like particle as a nanoplatform for biotechnology applications. *Journal of Materials Chemistry B,* **2023**, *11*, 6060-6074. DOI:10.1039/D3TB00318C

25. Huang, R. K. *et al*. The Prohead-I structure of bacteriophage HK97: implications for scaffold-mediated control of particle assembly and maturation. *Journal of Molecular Biology* **2011** *408*, 541–554. DOI:10.1016/j.jmb.2011.01.016

26. May, E. R.; Arora, K.; Brooks, C. L. pH-Induced Stability Switching of the Bacteriophage HK97 Maturation Pathway. *Journal of the American Chemical Society* **2014**, *136* (8), 3097-3107. DOI: 10.1021/ja410860n

27. Jia, Z.; Wong, L.; Davis, T.P.; Bulmus, V. One-Pot conversion of RAFT-generated multifunctional block copolymers of HPMA to Doxorubicin conjugated acid- and reductant-sensitive crosslinked micelles *Biomacromolecules.* **2008** *9* (11), 3106-13. DOI: 10.1021/bm800657e

28. Zeng, J.; Shirihai, O. S.; Grinstaff, M. W. Modulating lysosomal pH: a molecular and nanoscale materials design perspective. *Journal of Life Sciences (Westlake Village, Calif.)* **2020**, *2* (4), 25–37. DOI:10.36069/jols/20201204

29. Thorn, C. F.; Oshiro, C.; Marsh, S.; Hernandez-Boussard, T.; McLeod, H.; Klein, T. E.; Altman, R. B. Doxorubicin pathways: pharmacodynamics and adverse effects. *Pharmacogenetics and Genomics* **2011** *21*(7), 440–446. DOI:10.1097/FPC.0b013e32833ffb56